Optical coherence tomography: a review of clinical development from bench to bedside

Adam M. Zysk
University of Illinois at Urbana-Champaign
Beckman Institute for Advanced Science and
    Technology
Department of Electrical and Computer Engineering
Biophotonics Imaging Laboratory
405 North Mathews Avenue
Urbana, Illinois 61801

Freddy T. Nguyen
University of Illinois at Urbana-Champaign
Beckman Institute for Advanced Science and
    Technology
Department of Chemistry
College of Medicine
Biophotonics Imaging Laboratory
405 North Mathews Avenue
Urbana, Illinois 61801

Amy L. Oldenburg
Daniel L. Marks
University of Illinois at Urbana-Champaign
Beckman Institute for Advanced Science and
    Technology
Department of Electrical and Computer Engineering
Biophotonics Imaging Laboratory
405 North Mathews Avenue
Urbana, Illinois 61801

Stephen A. Boppart
Mills Breast Cancer Institute
Carle Foundation Hospital and Carle Clinic
    Association
Urbana, Illinois 61801
    and
University of Illinois at Urbana-Champaign
Beckman Institute for Advanced Science and
    Technology
Department of Electrical and Computer Engineering
Biophotonics Imaging Laboratory
405 North Mathews Avenue
Urbana, Illinois 61801
E-mail: boppart@uiuc.edu

Abstract. Since its introduction, optical coherence tomography (OCT) technology has advanced from the laboratory bench to the clinic and back again. Arising from the fields of low coherence interferometry and optical time- and frequency-domain reflectometry, OCT was initially demonstrated for retinal imaging and followed a unique path to commercialization for clinical use. Concurrently, significant technological advances were brought about from within the research community, including improved laser sources, beam delivery instruments, and detection schemes. While many of these technologies improved retinal imaging, they also allowed for the application of OCT to many new clinical areas. As a result, OCT has been clinically demonstrated in a diverse set of medical and surgical specialties, including gastroenterology, dermatology, cardiology, and oncology, among others. The lessons learned in the clinic are currently spurring a new set of advances in the laboratory that will again expand the clinical use of OCT by adding molecular sensitivity, improving image quality, and increasing acquisition speeds. This continuous cycle of laboratory development and clinical application has allowed the OCT technology to grow at a rapid rate and represents a unique model for the translation of biomedical optics to the patient bedside. This work presents a brief history of OCT development, reviews current clinical applications, discusses some clinical translation challenges, and reviews laboratory developments poised for future clinical application.
© *2007 Society of Photo-Optical Instrumentation Engineers.* [DOI: 10.1117/1.2793736]

1 Introduction

Optical coherence tomography (OCT) was first demonstrated for cross sectional retinal imaging in 1991 by a Massachusetts Institute of Technology (MIT) team headed by Fujimoto.[1] Since then, it has become a clinically useful diagnostic technique in the ophthalmology community. OCT instrumentation, buoyed by a stream of technological advancements, has undergone substantial improvement in the past decade, and, as a result, is now well positioned for wide adoption in various other clinical and research applications.[2,3] A number of promising scientific developments remain on the horizon as well, ensuring that the potential applications for OCT-based techniques will continue to widen for the foreseeable future.

OCT is an interferometric imaging technique that maps depth-wise reflections of near-infrared (NIR) light from tissue to form cross sectional images of morphological features at the micrometer scale. In the most basic form, an OCT instrument consists of a Michelson-type interferometer with a focused sample arm beam and a lateral-scanning mechanism. OCT traces its origins to the field of optical coherence-domain reflectometry, a 1-D distance mapping technique that was

Address all correspondence to Stephen Boppart, Mills Breast Cancer Institute, Carle Foundation Hospital, 611 West Park Street, Urbana, IL 61801 United States of America; Tel: 1–217–326–0283; Fax: 1–217–326–0285; E-mail: Stephen.Boppart@Carle.com

originally developed to localize reflections from faults in fiber optic networks and was quickly applied to biological applications.[4–6] These ties to the telecommunications industry have allowed the OCT community to leverage existing and state of the art low-cost hardware for biomedical applications.

Initial OCT technology was licensed by MIT to Humphrey Systems (now Carl Zeiss Meditec Incorporated, Dublin, California), which commercialized the technology for ophthalmic applications, released its first unit in 1996, gained Federal Drug Administration (FDA) clearance in 2002, and has sold more than 6000 of its Stratus OCT™ systems to date.[7] The OCT intellectual property landscape has become quite diverse since the development of this first system, with current patent holdings by a variety of corporate and academic entities. Among the approximately 40 U.S. patents with OCT in the title, Carl Zeiss Meditec still dominates corporate patent holders with more than ten, and the University of California leads academic institutions with four, as of the publication of this review. The corporate landscape itself is also expanding, and clinical OCT systems are now being manufactured for various applications by a group of established and start-up companies that includes Carl Zeiss Meditec Incorporated, LightLab Imaging (Westford, Massachusetts), Imalux Corporation (Cleveland, Ohio), ISIS Optronics GmbH (Mannheim, Germany), OCT Medical Imaging, Incorporated (Irvine, California), Novacam Technologies, Incorporated (Pointe-Claire, Canada), and Lantis Laser Incorporated (Denville, New Jersey). A new set of companies focusing on high-speed retinal imaging, including OptoVue, Incorporated (Fremont, California), Topcon Corporation (Tokyo, Japan), Optol Technology (Zawiercie, Poland), Heidelberg Engineering (Heidelberg, Germany), and Opthalmic Technologies, Incorporated (Toronto, Canada), has also emerged recently. Today, it is estimated that more than 37,000 OCT scans are performed daily in the U.S.[8]

In addition to the widespread development of clinical OCT systems, a significant market has also developed for research-targeted systems and components. For example, several companies, including Femtolasers Produktions GmbH (Vienna, Austria), Nippon Telegraph and Telephone Corporation (Tokyo, Japan), and Thorlabs, Incorporated (Newton, New Jersey), through its partner MenloSystems GmbH (Munich, Germany), sell compact broad-bandwidth optical sources that are marketed for OCT application. In addition, full-featured stand-alone OCT systems for research use are sold by Thorlabs, Incorporated and Bioptigen, Incorporated (Research Triangle Park, North Carolina), whose 840- and 1310-nm systems incorporate advanced visualization software and are compatible with a broad selection of application-specific scanners. This partnership between industry and academia has lowered the cost of entering the OCT research community. When coupled with the accessibility of ophthalmic OCT systems to clinicians, this commercialization has spurred exponential growth in both scientific and medical OCT research. A simple measure of this growth is the number of academic journal publications with OCT in the title. Figure 1 shows a graph of this metric over time, as measured using the U.S. National Library of Medicine PubMed service and the American Institute of Physics Scitation database, showing medical and scientific studies, respectively.

This surge in OCT investigations has taken place in parallel with the development of next-generation technologies that
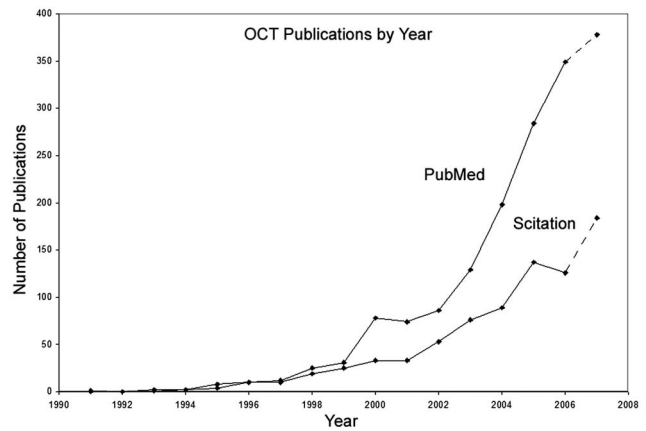

Fig. 1 Growth of OCT scientific and medical research publications. The graph shows the number of publications per year with optical coherence tomography in the title as indexed in the PubMed and Scitation databases. Data for 2007 is extrapolated based on the number of citations as of September, 2007.

have opened new frontiers of OCT application. High-speed imaging capabilities are key among these advances, as they have enabled the rapid acquisition rates that are often necessary to reduce artifacts due to patient motion. Additionally, these capabilities have led to the ability to generate 3-D volumetric images within reasonable time constraints. OCT imaging speed increases have been achieved with Fourier domain detection techniques such as spectral-domain OCT (SD-OCT) and swept-source OCT (SS-OCT), where rapid scanning of narrow-band source spectra is performed. These techniques have been made possible by technological advances in detector and source technologies. Finally, application of OCT deep within the body requires that minimally invasive imaging devices be employed since OCT penetration depths are typically limited to about 1 to 3 mm in highly scattering tissues. In addition to handheld probes, a variety of imaging devices have been integrated into clinical devices to allow for minimally invasive OCT imaging throughout the body with endoscopes, catheters, and biopsy needles.

2 Clinical Applications

2.1 *Ophthalmology*

OCT has made its most significant clinical contribution in the field of ophthalmology, where it has become a key diagnostic technology in the areas of retinal diseases and glaucoma.[9–12] Ophthalmic OCT imaging has not only made the transition from the bench to the bedside, but has also contributed to new laboratory investigations by revealing previously hidden clinical features of ocular diseases and the microscopic changes associated with treatment. The technique was first commercialized by Carl Zeiss Meditec, Incorporated and is now considered superior to the current standard of care for the evaluation of a number of retinal conditions.[13] Retinal OCT imaging provides high-resolution imagery of subsurface retinal features that were previously inaccessible with fluorescein angiography and ophthalmic ultrasound. The contrasting structure and reflectivity in the retinal layers allow for differentiation of the retinal nerve fiber layer (RNFL), nuclear lay-
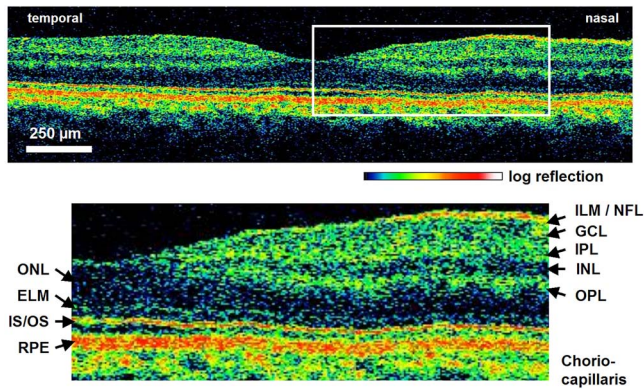
Fig. 2 High-resolution OCT images showing normal retinal structures at 3-μm axial resolution. Abbreviations: ILM—inner limiting membrane, NFL—nerve fiber layer, GCL—ganglion cell layer, IPL—inner plexiform layer, INL—inner nuclear layer, OPL—outer plexiform layer, ONL—outer nuclear layer, ELM—external limiting membrane, IS/OS—junction between the inner and outer photoreceptor segments, and RPE—retinal pigment epithelium. Images provided by Fujimoto and Drexler.

ers, plexiform layers, external limiting membrane, retinal pigment epithelium, photoreceptor layers, and choriocapillaris (Fig. 2). In OCT images of the retina, horizontal cell orientation is correlated with high reflectivity, while nuclei and vertical structures have low reflectivity.

OCT has been used to diagnose a number of vitreoretinal conditions. In addition to the evaluation of normal vitreous separation caused by aging,[14] OCT has been used to identify vitreous adhesions, which are thought to play a potential role in the development of macular holes and macular edema. The severity of macular holes, which are tears in the retina thought to be caused by shrinking vitreous that adheres to the retina, have been extensively investigated using OCT, greatly expanding the general understanding of the disorder.[10,15–18] These investigations are also crucial for patient care, especially in treatment planning, as surgical treatment decisions are dependent on the extent of damage. Postoperative management of macular hole repair is another powerful application for OCT imaging, which is capable of evaluating foveal features and monitoring for recurrent macular holes.[19–21]

Macular edema, a thickening and swelling occurring when fluid and protein deposits collect on or under the macula, is often a complication of diabetic retinopathy and can be caused by fluid leakage from abnormal blood vessels or traction by the vitreous gel. While fluorescein angiography remains the only method for the identification of leaking vessels, it cannot identify cases of nonvascular macular edema. OCT, however, has been extensively employed for the identification of cystoid macular edema and the monitoring of macular thickness, which is correlated to a decrease in central vision.[11,22–25] Finally, in age-related macular degeneration patients, OCT has been used to assess the vitreoretinal interface and macular attachment, identify the presence of intraretinal cysts, and evaluate the subretinal space.[26]

Analysis of RNFL thickness, which is thought to be a sensitive indicator of glaucomatous damage, has also been undertaken with OCT.[27,28] In comparison to traditional analysis, which was not capable of assessing diffuse atrophy, commer-

cial OCT systems, which are now equipped with automated software that allows for quantification of RFNL thickness over wide retinal areas, are capable of precise, reproducible measurements.[29–33] Studies have shown that these measurements are highly correlated with visual function.[34,35] Additionally, RFNL thickness measurements allow identification of focal defects in earlier stages of glaucoma development than standard techniques.[33,36] The extensive body of investigative work that has been performed in this area has revealed a strong potential for routine glaucomatous damage assessment using OCT-measured RNFL thickness. Various other ophthalmic OCT applications have also been investigated, including the visualization of lamellar holes, assessment of vitreomacular traction syndrome,[37] and measurement of corneal water concentration *in vitro*.[38]

OCT has also been used to evaluate chorioretinal disease treatment protocols.[39–41] Pharmacological treatment approaches, including intravitreal drug injections, have been the topic of several recent studies that incorporated OCT imaging.[42,43] These imaging studies have provided powerful visual evidence that drug injections may be preferable to photothermal tissue ablation in certain circumstances. Several additional randomized clinical studies are underway to evaluate laser and pharmacological treatments for macular diseases. These investigations demonstrate the increasing tendency to incorporate OCT imaging, as opposed to angiography alone, into clinical studies, due primarily to its ability to capture treatment-induced retinal changes on the micrometer scale.[44–46]

Several recent technological advancements have been applied to retinal imaging. High-speed 3-D OCT retinal imaging, for example, significantly reduces movement-induced artifacts during scans across wide regions.[47] The spectral-domain detection techniques that enable high-speed imaging have recently been incorporated into a number of commercial systems. Polarization-sensitive OCT (PS-OCT) is a functional OCT technique that reveals sample-induced polarization changes in the optical field. This technique has been used to map optical retardation and slow-axis orientation in the retina, and to identify a polarization-scrambling layer at the posterior boundary of the retina that is thought to be the retinal pigment epithelium.[48,49] Adaptive optics have also been employed in retinal imaging to correct for wavefront distortions induced by ocular aberrations at the air-cornea interface.[50,51] These techniques compensate for this distortion by employing specialized cameras to account for defocus and astigmatism. These techniques, which often require highly complex optical systems, have shown a significant improvement in resolution over standard OCT imaging, even enabling the visualization of individual photoreceptors. Another significant recent advance is the incorporation of functional information to OCT imaging, a modality referred to as optophysiology, wherein changes in dark-adapted retina caused by light stimulation result in pronounced local variation of the tissue reflectivity profile in the inner/outer segments of the photoreceptor layer and the plexiform layers. The technique could significantly improve the diagnosis of various ophthalmic conditions that have functional vision impairment but lack associated morphological changes, potentially leading to a better understanding of retinal physiology and pathology.[52]
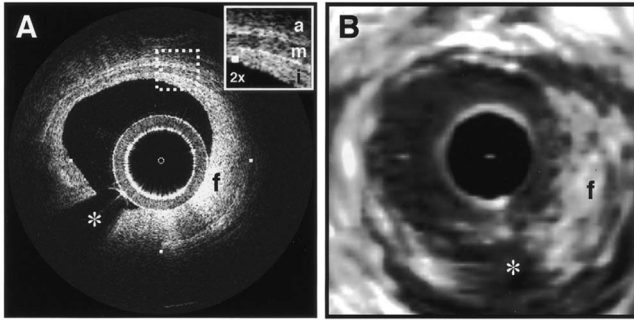
Fig. 3 Intravascular imaging of a fibrous coronary plaque showing: *i*—intimia (with intimial hyperplasia), *m*—media, and *a*—adventitia. The left figure is an intravascular OCT image showing a clear delineation of layers, including the internal and external elastic laminea. A fibrous plaque (*f*) is visible and partially obscured by a guidewire shadow artifact (*). The right figure is a corresponding 30-MHz IVUS image at the same location.[62] Reprinted with permission. Copyright Elsevier, 2002.

2.2 Cardiology

Over the past decade, OCT has been extensively applied in the field of cardiology. It was first used to examine the structural integrity of the vasculature in the coronary artery, and more recently has been applied for cellular and molecular analysis using modalities such as spectroscopic OCT and PS-OCT.[53–71] There have been several technological advances that have allowed OCT to become adaptable for imaging the cardiovasculature, including the development of rotational catheter-based probes, the improvement of acquisition speed, and the introduction of functional OCT modalities. As these technological advances have been made, imaging and validation have been performed *in vivo*.

In comparison to intravascular ultrasound (IVUS), OCT provides higher resolution by approximately an order of magnitude (Fig. 3).[55,57,59,62] In addition, probes have been developed to integrate OCT sample-arm optics into intravascular catheters, providing forward and radial OCT imaging capabilities.[65,72] Catheter-based imaging, enabled by high-speed data acquisition systems,[73] can be performed by either manually feeding the probe through the vasculature or automatically pulling it through the vasculature during image acquisition.

Atherosclerosis is the process in which materials such as cellular waste, fatty substances, cholesterol, calcium, and fibrin build on the inner lining of an artery, or in regions surrounding the lumen. Atherosclerosis currently accounts for more than 75% of cardiovascular diseases (CVDs) including strokes, which make up 18% of CVDs.[74] The development of vulnerable plaques is often caused by an inflammatory response and is a key component in the development of atherosclerosis and of CVDs in general. Recent research has focused not only on the detection of plaques but also on their potential for rupture. Distinguishing characteristics of vulnerable plaques include a thin fibrous cap, a large lipid pool, and an increase in macrophage activity.

The ability to identify the location and progression of atherosclerotic lesions has become a critical issue, since they are a leading cause of death and severe long-term disability.[74] An ideal clinical application for cardiovascular OCT imaging is

the visualization of vulnerable plaques in the coronary or carotid arteries, and evaluation of their potential for progression or rupture. This evaluation would ideally be performed after these suspicious areas had been localized regionally by another method like CT, ultrasound, or fluoroscopy. Structural OCT images penetrate about 1 to 3 mm into tissue and have been correlated with IVUS images, the current standard in intracoronary imaging.[62] Intravascular OCT imaging is limited by tissue penetration depth and blood-induced signal attenuation, which can be reduced with a saline flush or temporary vascular balloon occlusion prior to imaging.

OCT has been demonstrated as a tool for *in vivo* quantification of activated macrophage content and identification of plaque type contained in a lesion.[69,75] Plaque identification has been demonstrated with high sensitivity and specificity (fibrous 87%, 97%; fibrocalcific 95%, 100%; and lipid-rich 92%, 94%). The OCT-quantified macrophage density underneath the fibrous cap has been shown to directly correlate with the patient's clinical presentation. The presence of activated macrophages located near the endothelial layer is thought to contribute to the instability of a vulnerable plaque by tissue factor expression and the erosion of the endothelial layer.[68,75,76] In addition to the presence of macrophages, clinically interesting materials include calcific nodules associated with plaque thrombosis, multinucleated macrophages, and cholesterol crystals present in lipid pools. These materials are being investigated with OCT, and preliminary results validate the ability to detect and identify plaques and to assess associated risk factors.[62,69,75] In addition, OCT has been used to characterize the attenuation and layer thickness changes associated with arterial wall components such as the intima, media, lipid-rich regions, and calcifications.[77–80]

Intravascular OCT has been successfully used in the characterization and visualization of cardiac interventions, such as percutaneous coronary intervention and stent implantations.[53,56–58,62,64,68,69] The most common cause of procedural failure in the treatment of chronic total occlusion (CTO) by percutaneous coronary intervention is the inability to properly navigate the guidewire. In cases of CTO of a coronary artery, OCT is being evaluated as a tool to decrease the chances of guidewire perforation of the artery and dissection of the intima.[81,82] In the case of stent implantation, imaging has been performed prior to balloon deployment and after stent installation, giving surgeons a real-time assessment of stent apposition and its role in re-expanding the vascular walls.[54,61] OCT was also recently used to visualize several features that could not be observed using IVUS, including stent integrity, neointimal proliferation, and neovascularization.[77,83,84] The high-resolution *in-vivo* OCT images allowed for a real-time assessment of the optimal placement and deployment of stents by allowing for assessment of stent overexpansion and identification of poststenting vessel injuries.[54,85] In addition, OCT has been used to view neointimal hyperplasia resulting from coronary drug-eluting stent implantation. Finally, high-resolution OCT imaging has been applied for the assessment of stent failures such as restenosis and stent thrombosis.

Recent efforts to develop functional OCT modalities[86–96] have allowed cardiovascular imaging to progress beyond morphological sensitivity. These OCT techniques are helping to bridge the gap between the structural and underlying bio-

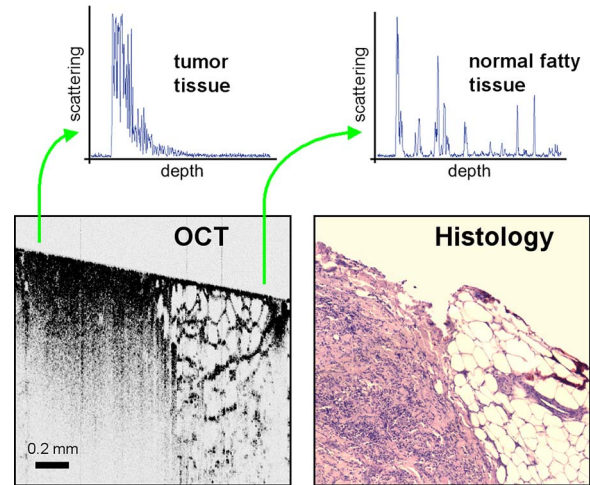**Fig. 4** A clinical vascular OCT system from LightLab Imaging.

Fig. 5 OCT imaging of the human breast. The bottom images are of an excised human breast tumor showing the margin between invasive ductal carcinoma (left side) and normal fatty tissue (right side). The OCT and hematoxylin and eosin stained histological section correspond well. Axial scans from the two tissue types (top) show the changes in tissue density and separation between scattering features.

chemical information that may lead to improved understanding and assessment of disease. PS-OCT, for example, is a functional mode of OCT[92] that has shown potential in the study of vulnerable plaques. Changes in intrinsic tissue birefringence are thought to be indicative of changes in the tissue functionality and structure. Some preliminary studies show that fibrous and calcified plaques have unique birefringence properties that can be visualized with PS-OCT. Also, the concentration of collagen rather than the collagen type was found to dominate overall plaque birefringence.[97] Since the reduced synthesis of collagen and the increased expression of collagenase are associated with the development of vulnerable plaques, it is hypothesized that the accompanied loss of birefringence will be detectable with PS-OCT. In the event of an accumulation of collagen leading to vascular stenosis, PS-OCT may also be able to detect the associated increase in birefringence.[97,98] OCT can also be used to measure the intrinsic optical attenuation coefficient of tissue *in situ*.[99] This capability may allow for spatial discrimination between thrombus, lipid-rich regions, intimal tissue, calcified tissue, and medial tissue.[79,80,100] Other functional modalities like optical coherence tomographic elastography, sometimes referred to as optical coherence elastography, are also being investigated to evaluate the mechanical properties of arterial walls.[101,102]

Intravascular OCT has begun to move from the validation phase to clinical use. For example, the effects of focal and multifocal macrophage distribution have been studied in patient populations at the Massachusetts General Hospital.[75] These studies demonstrate the progression of OCT imaging

from the bench to the bedside and back, through the direct clinical impact on patient care and the research contribution of OCT-generated insights into the pathogenesis of coronary diseases. Finally, commercial OCT systems, including those developed by LightLab Imaging, are being targeted to the cardiovascular market, primarily aiming to more precisely direct conventional balloon angioplasty and stent procedures. LightLab Imaging has installed 80 intravascular OCT imaging systems (Fig. 4), completed a 100-patient U.S. Food and Drug Administration (FDA) trial, and obtained regulatory approvals for cardiology imaging in the European Union, China, and Korea.

2.3 Oncology

OCT application in the field of oncology is a relatively recent development. Despite the short time since development, imaging has been performed on a broad spectrum of malignancies including those arising in the breast, bladder, brain, gastrointestinal, respiratory, and reproductive tracts, skin, ear, nose, and throat. OCT imaging has largely been applied for the evaluation of surgical margins and the early detection of small lesions that would often not be visible on gross examination, two tasks that align well with current clinical emphases on early detection and intervention.

First demonstrated in rat mammary tumor models,[103] OCT has the potential to be an effective tool for the detection of lesions in the human breast due to the significant structural differences between the fibro-fatty tissue comprising most of the breast, and the densely scattering tumor tissue that arises from within the functional epithelial network of ducts and lobules (Fig. 5). By analyzing the spatial frequency content of the axial scattering response, highly sensitive tissue classification has been shown with normal tissue and invasive ductal carcinoma lesions.[104] The internal location of most breast lesions limits OCT application to open surgical procedures or requires the use of needle-based imaging devices.

In the operating room, OCT has been used to scan recently excised breast tissue during lumpectomy procedures to assess the margin of normal tissue surrounding the tumor. Typical procedures call for initial gross pathological evaluation of the mass, followed by light microscopy of frozen or paraffin-embedded tissue sections. Not only is this procedure time and labor intensive, but it also suffers from a number of potential problems, including limited spatial sampling over the mass, seepage of ink deposited during gross examination, and artifacts induced by radiographic manipulation.[105] By imaging the top 1 to 2 mm of the entire tissue surface immediately on resection, the margin status can be assessed quickly and thoroughly with OCT, enabling the surgeon to resect additional tissue immediately, if necessary.[106]

OCT has also been investigated as an adjunct to the standard sentinel lymph node biopsy (SLNB) procedure used to map the lymphatic system and determine whether a primary breast tumor has metastasized.[107] By using dyes or radioactive tracers to locate the first node in the lymphatic drainage pattern leading away from the tumor site, the SLNB procedure drastically reduces the number of lymph node resections required for accurate histopathological staging of the disease. OCT may be applied *in vivo* to provide real-time detection and indicate the necessity of additional surgical resection.

Breast biopsy procedures, used to physically sample suspicious tissue without open surgery, may also be improved by incorporating OCT-based instrumentation. Significant sampling difficulties have been reported when guiding needle biopsies with external ultrasound and x-ray imaging techniques, as is the current standard practice. By incorporating a biopsy needle device into the OCT sample arm, additional diagnostic information can be generated, aiding in the identification of the appropriate tissue for biopsy. Single axial scans can be acquired using focusing micro-optics at the tip of a single-mode optical fiber, potentially providing diagnostically significant backscattering and refractive-index information from a device that can be easily incorporated into a standard biopsy needle.[108–111]

Ear, nose, and throat and esophageal lesions are another set of promising targets for OCT imaging due to the difficulties presented by traditional visual examination and the accessibility of tissue using specialized endoscopic OCT techniques.[112–114] OCT has been used to evaluate the laryngeal mucosa,[115] the most common site of primary head and neck malignancy development, and has been found to be an effective means of quantifying the thickness of the epithelium, evaluating the integrity of the basement membrane, and visualizing the structure of the lamina propria.[116,117] In addition, preliminary studies have been conducted to evaluate the application of OCT imaging to the oral cavity, oropharynx, vocal folds, and nasal mucosa.[118–120]

OCT has also been extensively applied in the gastrointestinal tract.[121–124] Patients with Barrett's esophagus, a condition of cellular metaplasia that can progress to esophageal adenocarcinoma, typically undergo regular endoscopic surveillance and biopsy to monitor for dysplastic changes. A number of studies[125–132] have been conducted to determine the feasibility of using OCT imaging to identify suspicious lesions, including a recent blinded clinical trial that showed an accuracy of 78% for the OCT detection of dysplasia in patients with Barrett's esophagus.[127] While some improvements in clinician training, feature definition, and system resolution are still needed, this OCT application is a strong candidate for future clinical adoption. Finally, advances in the analysis of angle-resolved axial-scan data for the evaluation of scatterer size have been applied for the evaluation of nuclear morphology, generating promising results for detecting dysplasia in an animal model.[133]

Recently, promising advances have also been made in the detection of cervical cancer with OCT. *In-vivo* pilot studies have shown that in premenopausal women, average OCT reflection intensities from abnormal cervical epithelium were significantly stronger than normal epithelium, and vice versa in postmenopausal women.[109,134] These differences are likely due to well-characterized neoplastic changes in the chromatin texture and the nuclear morphology and texture.[135] Scattering changes have been incorporated into algorithmic tools developed for the identification of unique pathologies by fitting experimental data to layered media models simulated within the framework of small-angle radiative transfer approximations.[136]

In addition to these academic investigations of OCT in oncology, several applications have also been embraced by commercial system developers. Imalux Corporation, for example, has built on significant academic research,[137–145] and is targeting the detection of bladder cancer, among other applications. OCT is thought to be valuable as an adjunct to traditional cystoscopy and laparoscopy procedures (Fig. 6). In transurethral resection of bladder tumors, for example, OCT has the potential to eliminate local recurrence and minimize the amount of normal tissue removed by guiding surgical resection lines. Another commercially targeted application is dermatological evaluation, a field in which OCT is well established for cross sectional visualization of the dermis, epidermis, adnexal structures, blood vessels, and boundaries of cancerous lesions (Fig. 7).[146–148] Although general-purpose OCT systems can easily target the skin, ISIS Optronics has developed a commercial OCT system that is specifically tailored to dermatology applications, allowing for both scattering and refractive index mapping.

2.4 Other Applications

New applications for OCT are constantly being developed outside of the fields of ophthalmology, cardiology, and oncology. Noteworthy developments include the investigation of OCT and PS-OCT for the evaluation of musculoskeletal tissues,[149–151] the quantitative mapping of the upper airway size and shape,[152,153] and the visualization of dental structures.[154,155] Dental OCT, capable of detecting early decay not visible on standard x-ray, is being developed commercially by Lantis Laser Incorporated, which has secured intellectual property rights, has raised significant funding, and is in the process of designing a specialized clinical system. Additionally, applications in areas such as neurological, ovarian, and prostate imaging continue to advance, but are not yet ready for clinical use. OCT image-guided procedures continue to affect patient care by moving diagnostic procedures out of the laboratory and to the point of care.
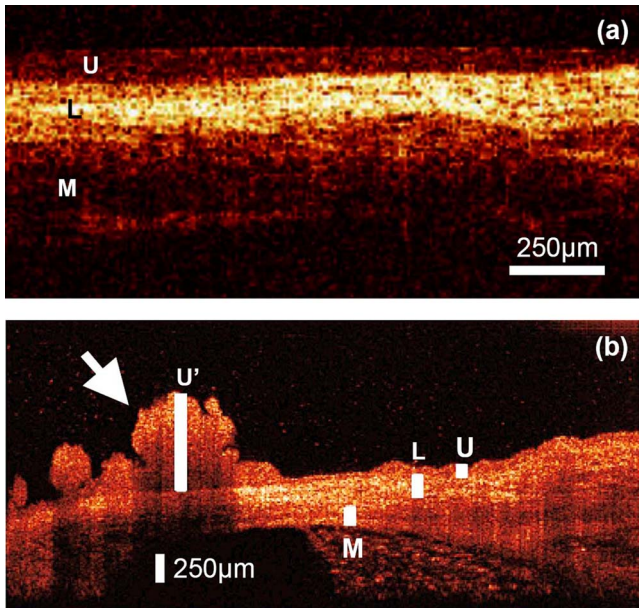
Fig. 6 (a) High magnification OCT image of benign human bladder taken with a clinical system during cystoscopy. Three distinct layers are visible: urothelium (U), lamina propria (L), and muscularis propria (M). A sharp border is visible between the urothelium and the lamina propria. Image provided by the Imalux Corporation, courtesy of Manyak (George Washington University, Washington DC). (b) Low-magnification OCT image of a neoplastic rat bladder taken with a research system. The diseased urothelium (U′, arrow) is clearly visible. Reprinted with permission (labels modified). Copyright Optical Society of America, 2002.

3 Clinical Translation

Similarly to the developmental process for pharmaceutical agents, there are five developmental steps that a new medical imaging technique takes as it is developed from the laboratory bench to the bedside (Fig. 8).[156] Step 0 is focused on technology development in the laboratory through initial design, calibration, and testing. About five years is typically spent on this step. Step 1 involves pilot studies that are carried out to assess the feasibility and safety of the technique for the clinical application of interest. During this step, the criteria or methods used to differentiate between normal and abnormal tissue are evaluated. As these studies gain momentum and provide promising results, research moves on to Step 2, which is a limited trial to study the usefulness of the technique in distinguishing between normal and abnormal tissue or in grading different disease states. In Step 3, technology standardization is of critical importance as multicenter randomized clinical trials begin. This is the ultimate validation of the optical imaging modality in a clinical environment. About ten years are typically spent in Steps 1 to 3 to fully translate a technology from the bench to the bedside. Finally, in Step 4 the new imaging modality is adopted as the standard of care, and is further commercialized for the clinical specialty of interest. This 15 to 20 year process can be further extended by the introduction of contrast agents or other exogenous agents.

3.1 Imaging Validation

Throughout the translation process, there is continuous feedback between tissue phantom studies, cell line studies, animal
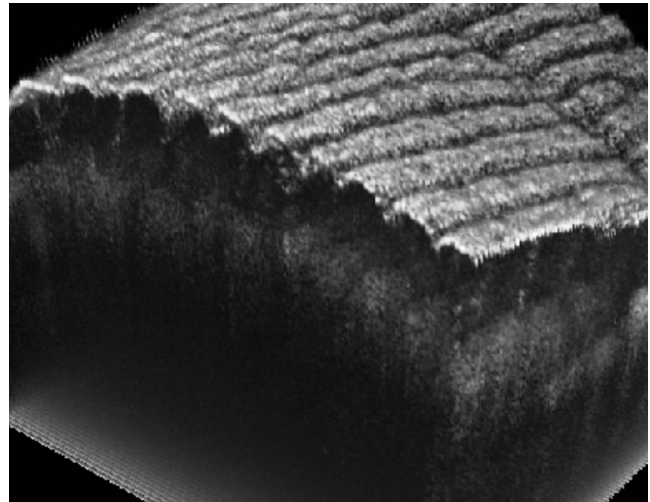

Fig. 7 3-D OCT data volume showing the morphology of a human finger pad. Finger print ridges, dermal layers, and sweat glands are visible. Scanning depth is 2 mm. Image provided by Bioptigen, Incorporated.

studies, and human subject studies. The performance of an imaging system must be continuously evaluated using these investigation methods.

In OCT, tissue phantoms, broadly defined as samples designed to mimic human tissue, may model the optical properties of tissue by incorporating scatterers and absorbers. They may also be constructed to model the mechanical and spatial properties of tissue through the use of scaffolds or gels. More advanced phantoms may incorporate the use of cell lines such as cardiomyocytes, fibroblasts, and cancer cells. Grown in cell scaffolds, these phantoms are often used to identify biological components that are overexpressed in a disease of interest and to investigate their contribution to observed OCT signals.

Ex-vivo tissue specimens can be obtained from either well-characterized animal models or human patients. A number of appropriate animal models exist for human diseases. For example, N-methyl-N-nitrosourea (MNU) -induced rat mammary tumors model human ductal carcinoma, and atherogenic rabbit diets induce atherosclerotic lesions similar to those in humans. Human tissue specimens may be available from local medical institutions in the form of discarded pathology specimens or from tissue banks and repositories[157,158] run by medical centers, hospital consortiums, or governmental agencies such as the United States National Institutes of Health. As OCT system designs have become more portable, many *in-vivo* imaging opportunities have become available. A number of unique issues are introduced during *in-vivo* testing such as motion artifacts, the mechanical properties of tissue, the physical location and frequent inaccessibility of the *in-vivo* tissue, the presence of additional biological components not present in tissue phantoms or *ex-vivo* samples such as blood, fluid from saline washings, cauterized or scar tissue, and finally, the new logistics of incorporating new hardware and technology into clinical protocols and settings.

Tissue validation studies are typically compared with light microscopy of histological sections, the medical gold standard. Histological evaluation itself has a degree of uncertainty, however, since pathological diagnoses suffer from
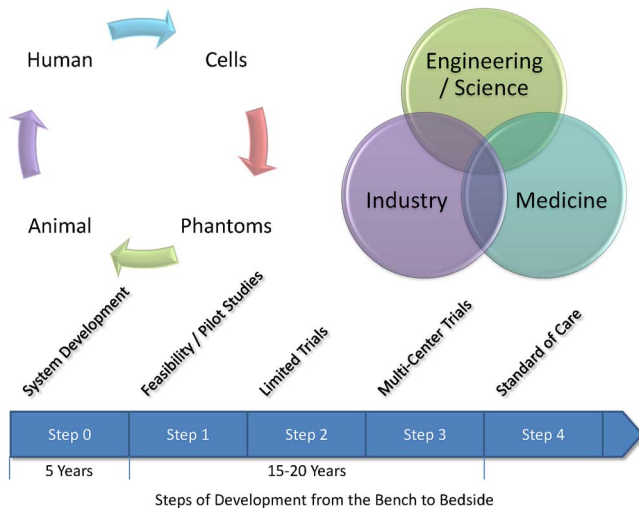
Fig. 8 Diagram of the translational steps. The focus is on validation within the first phases of development. The focus shifts to interaction with the other groups as development moves toward clinical trials, acceptance into medical community, and commercialization.

sampling variability and interobserver variability.[159] For example, if a pathologist is uncertain as to the grade of dysplasia present in a sample, he or she may obtain a second or third opinion to provide a consensus diagnosis. This type of analysis is highly dependent on pathologist experience, suggesting that the diagnosis process is expert based, rather than evidence based.[160] Imaging modalities, on the other hand, rely on quantitative, or evidence-based, methods to distinguish between tissue types.

Additional issues also arise when tissue specimen treatment is considered. Histopathological examination typically requires that the tissue be excised, preserved in formalin, embedded in paraffin wax, thinly sliced, and stained prior to examination. It is clear that significant morphological artifacts may be induced as a result of this processing, and that the histological sections may not truly reflect the structural features *in vivo*. It is also recognized that a number of optically induced artifacts arise in OCT images. The high degree of correlation between OCT images and histological sections remains remarkable, considering that images from each technique are generated by the transmission of light from orthogonal directions. Still, the diagnostic usefulness of histopathology and OCT stems from the ability of each to detect deviations from established baseline image features that arise from normal morphology. These issues raise a logical question: is histology the most appropriate standard to which OCT imaging should be compared? In the case of structural OCT, histopathology is likely the most appropriate method for evaluation of morphological features, despite these issues. However, as OCT incorporates molecular sensitivity and functional imaging, this may no longer hold true. Ultimately, one means by which to bypass the discrepancies between *in-vivo* imaging and histopathologic evaluation is to employ evidence-based medical outcome investigations such as randomized clinical trials, which further validate the use of OCT in clinical and surgical practice.

Imaging techniques are primarily developed for their diagnostic capabilities. There are four stages of technology vali-

dation for assessment of the utility of a diagnostic test.[161–163] In the first stage, test results are assessed for their ability to show differences between patients with and without a specific disease or disorder. Stage two studies aim to ensure that all patients with the disease yield abnormal test results, while stage three studies evaluate test results for the ability to differentiate between patients with and without the disorder. Finally, the fourth stage assesses the effect of early treatment on patients who were diagnosed using the test. This validation process requires the incorporation of animal and human tissues into the research environment.

3.2 *Animal and Human Studies*

In the United States, studies involving the use of animal or human tissue require compliance with federal and state laws that regulate the humane use of animals and the rights of human subjects. At most institutions, two oversight committees exist: the Institutional Animal Care and Use Committee (IACUC) and the Institutional Review Board (IRB). These committees review and approve all research studies involving the use of animals and human subjects, respectively, prior to initiation. The use of research animals in the U.S. is primarily regulated under the Animal Welfare Act[164] and the Health Research Extension Act,[165] which specifies IACUC committee membership requirements that strive to represent the interests of researchers, animals, and the community at large.

IACUC protocols address issues such as the study rationale, the justification of animal use, and the number of animals to be used. The protocol evaluation time frame varies by institution, but often takes on the order of 1 to 3 months, requiring that protocols be developed well in advance of the intended start of research. Many institutions also have an enforcement arm that is responsible for maintaining the well being of research animals by providing animal care services and performing inspections of protocol compliance. Finally, individual funding agencies often have separate requirements and guidelines regarding the proper use of research animals.[165]

Studies involving human subjects face similar regulations. The primary responsibility of an IRB is to protect the rights of participating human subjects by regulating patient consent procedures and the protection of personal information. Informed consent protocols require that, only after potential study subjects are fully informed and fully understand the research study, can they voluntarily consent to participation. Proper informed consent includes information on investigators, a layman's explanation of the research, and a clear description of the proposed procedures. Additionally, the potential personal and societal risks and benefits of the research must be presented.

The personal health information of enrolled patients must also be protected, a process that can be complex when attempting to correlate research results with clinical test results. Investigators often require access to diagnostic information regarding disease state and, in the case of OCT, direct correlation between OCT images and histological sections from the imaged area are typically necessary for validation. Medical records and privacy are protected under the Health Insurance Portability and Accountability Act[166] that preserves patient confidentiality by requiring the use of code sets or keys to

deidentify medical information that is made available to researchers. Records to be released under these provisions must be detailed in the informed consent document.

IRB membership and protocols are subject to U.S. federal regulation. Protocols may be classified as exempt research, expedited review research, or full board review research based on the nature and location of the research. Most optical imaging research studies undergo expedited review by IRB members due to the minimal risks involved, especially in the case of *ex-vivo* studies. Minimally invasive OCT protocols, such as intravascular or gastrointestinal tract studies, are likely to undergo full review by the entire board. With the exception of exempt research, continuing reviews are conducted every 6 to 12 months to evaluate the progress of the research study, the impact of adverse events, any protocol changes, and any changes in the risks/benefits balance.

Safety protocols and training are also required for those handling biohazardous materials from animal or human subjects. In addition to institutional human subject training, the U.S. National Institutes of Health (NIH) offer web-based training modules. This training generally covers regulation history and justification, in addition to presenting information on unethical human research and informed consent.

3.3 Clinical System Design

Once the fundamental technology has been tested or proven in a laboratory setting during translation Step 0, imaging instrument hardware and software must be adapted for compatibility with the clinical setting in which it will be used. Many issues must be taken into account, including the size, stability, and ease of use of the instrument, the acquisition and processing speeds of the system, and the accessibility and sterility of any probes that may be in close proximity to or come in contact with tissue. In addition, instrument and data standardization is critical to aiding physicians and researchers in system operation and image evaluation. As OCT continues to be developed for new applications, standardization among investigators and across locations would be of significant benefit to the community.

Since OCT can be implemented in a fiber-based system, construction of the optical components of a portable OCT system is rather straightforward. Recent advances in compact light sources and detectors have allowed the footprint of such a system to shrink significantly, an important factor to consider, since many clinical settings have minimal available space. Issues of stability and ease of use are also of critical importance when an OCT system is to be used in demanding environments that require the system to be operational within minutes of being initialized. In this case, the optical system must maintain its optical alignment, or be rapidly realigned, following frequent movements within the hospital environment.

Recent advances in OCT detection schemes have enabled axial-scan acquisition speeds on the order of hundreds of kilohertz. This capability necessitates the implementation of high-speed data processing hardware and software that are capable of incorporating new computational algorithms that compensate for dispersion and beam focusing aberrations. These requirements can be met by using digital signal processing units, multiple processors, or parallel computing schemes.

The sample arm of an OCT system can range from a handheld scanning probe to a fiber-based probe used in a catheter, endoscope, or biopsy needle. In surgical applications, probes used outside of the sterile surgical field may be easily sterilized with a bleach solution and disinfected after contact with biological materials. To alleviate the need for repeated sterilization and also as an economic incentive, probes can be made as single-use disposable medical devices, given the relatively low cost associated with the optical components. Fiber-based probes, for instance, are often constructed so that the optical components do not come in direct contact with the tissue but are protected by a transparent sheath, or a metal sheath with a clear window for the imaging beam. Handheld probes with sufficiently long working distances can also be easily protected by covering them with disposable sterile plastic wraps. While these methods are sufficient for *ex-vivo* use, *in-vivo* applications have more rigorous requirements. Sterile plastic covers may still be used for handheld probes, but fiber-based probes must either be disposable after a single use or be able to withstand sterilization in an autoclave, a device that exposes materials to high temperature steam.

Clinical data can be expected to vary across patients, tissue specimens, diagnoses, and imaging systems. System standardization and calibration procedures can reduce system-induced effects. For example, measuring the system's signal-to-noise ratio or imaging a standard tissue phantom prior to an imaging session can be useful for system alignment and the comparison of image quality over time. Other forms of variability, such as specimen or patient health and state of disease, may be overcome by recruiting a sufficient number of study participants to achieve appropriate statistical power.

Software standardization is also a significant issue, since many research teams develop unique software to control systems, acquire data, and analyze images.[167] No standard image or visualization formats currently exist in the OCT research community. Data standardization would bring benefits in data interpretation from multiple sites and make algorithm development and data analysis easier to apply retroactively. An equally important issue is the definition of the role that OCT data will play in the clinical applications of interest. For example, if OCT will compliment that of another imaging modality, one must consider the means by which OCT results will be merged with existing acquisition techniques, data storage systems, and visualization methods. Efforts are underway by the NIH and industry groups to establish a standard for optical imaging technologies.[167] Development of an open source platform is also underway, potentially allowing modalities to become "plug-ins," potentially providing standardization and reduced software development requirement on the part of individual investigators.

Medical instruments typically must undergo testing prior to hospital use to ensure that operation will not interfere with the clinical environment. For example, electromagnetic interference with other equipment must be ruled out, electrical power quality requirements must be insured, and laser radiation must be kept at safe levels. The latter issue is of little concern for clinical OCT systems that expose the sample to less than a few milliwatts of power, most often falling well under the laser radiation maximum permissible exposure lim-

its set forth under ANSI laser safety standards for skin and soft-tissue exposure.[168] Attenuation of the incident power is frequently needed to meet the safety requirements for ophthalmic OCT imaging.

Future issues to be addressed include the incorporation of OCT results into medical records and assignment of clinical responsibility for the acquisition and interpretation of the OCT results within the medical team. Increased data acquisition rates generate very large OCT datasets that must be properly stored and analyzed. It is also evident that new approaches for computer-based detection algorithms will become important as the acquired data volume exceeds the ability of users to extract diagnostically useful information in relatively short periods of time.

3.4 Clinical Trials and Commercialization

Randomized clinical trials form the basis of evidence-based medicine and are conducted in four phases. In phase 1 trials, the technology is applied to a small group of individuals to evaluate its safety and to identify any potential issues or side effects. Phase 2 trials are expanded to a larger group of patients, further testing the effectiveness and safety of the technology. Phase 3 trials are traditionally multicenter studies and are carried out to confirm the effectiveness of the new technology, compare it to other commonly used diagnostic methods, and collect any information on anomalies or adverse effects that may occur as side effects. Phase 4 trials are almost always carried out by the private sector in an effort to determine the risks, benefits, and optimal uses of the technology.

In the late stages of development and in clinical trials, private sector individuals with specializations in biomedical imaging technologies are often introduced for guidance and funding. Corporate partners frequently prefer to pursue technologies with established manufacturing processes that are easily scalable and transferable, rather than investing in fundamental research and development. Major medical companies also primarily focus investments on technologies with demonstrated clinical success and strong market potential.

Before a technology can be fertile for commercialization, it must be tied to a specific procedure rather than simply a clinical field of application. The tight restrictions surrounding device approval as part of the standard of care require that the approved uses be well developed and validated. Only successful clinical trials will yield clinical adoption of new technologies and, in the U.S., the necessary premarket approval by the FDA.

Currently, the burden of clinical trial costs is shared by the academic community and the private sector. There are currently no reimbursements available from the U.S. Centers for Medicare and Medicaid Services (CMS) for technology evaluation, as physician reimbursement rates have not kept up with rising medical costs and are expected to decline in the near future. Reimbursements made for clinical imaging trials would most likely take away from funds allocated to other diagnostic or screening procedures. Standardization of optical imaging validation processes may assist the community in gaining FDA approval and potential CMS reimbursement.[169]

3.5 Barriers to Translation

The barriers of translation[156] can be separated into cultural and logistical challenges. Cultural challenges arise due to differences in communication and career expectations. The clinical language of medicine is often not intuitive to the scientists and engineers focused on basic research. The opposite is also true as scientists and engineers find it difficult to explain their research to physicians. Additional cultural barriers exist between the academic professional community (medical, basic science, or technology research) and the more clinical (nonresearch) medical professionals. For example, scientists are often focused on the discovery and development of new technologies, while physicians are focused on how to best treat patients or help introduce new techniques to benefit patients. Institutional expectations for career development also tend to be quite different, often leading to mismatches in research translation goals and focus. There is clearly a role for physician-scientists or physician-engineers to break down these cultural barriers, as these individuals have been trained for the specific purpose of translating the basic science or technology research into the clinic, helping to bridge the gap between these communities.

The remaining barriers are logistical in nature. First, geographic limitations may create barriers to collaboration. The research campuses where biomedical optics research is conducted are often located far from the medical campuses or the institutions where patient care is delivered. The difficulties presented by this scenario may be overcome by creating physical space at both locations where visitors can be embedded, potentially opening new lines of communication and collaboration. Institutions with medical and university campuses located within close proximity of one another, however, have a distinct advantage when pursuing technology translation.

The legal implications of collaborations occurring across multiple institutions can be complex. In the U.S., the Bayh-Dole Act gives universities intellectual property control over federally funded research. Though the effects of this legislation are widely debated, it may potentially act to impede the flow of scientific discovery by pressuring institutions to devote resources to the development and commercialization of intellectual property. By increasing the involvement of the private sector in clinical trials, however, technology development barriers may also be reduced as funding is potentially increased.

Operational and navigational barriers also exist. The introduction of a new medical imaging technology increases the need for trained users of a nonstandard technology, for robust and reliable instrumentation, for interpreters of nonstandard data, for duplication of the technology, and for the establishment of standard operating procedures. Finally, a wealth of specialized knowledge is needed to navigate through the complex landscape of study design, federal regulations, oversight committees, patient recruitment and consent, outcome measures, legal implications, and commercialization requirements.

Many of these challenges can be overcome through the involvement of all stakeholders in the development and translation of a technology. This cooperation will open lines of communication between the various parties and thereby speed translation, especially in the early phases of technology devel-

opment. Feedback about upcoming or potential issues can be obtained early in the translation process, assisting scientists and engineers as they maneuver through the process. The establishment of physical and interpersonal infrastructures may assist researchers to navigate the complicated technology translation landscape. Mentorship networks and physical infrastructure may be developed for patient recruitment, team member communication, data analysis, data sharing, and regulation compliance. Other proposals have called for increased funding for the standardization, duplication, and validation processes.

Finally, networks and teams of independent investigators often form in the medical research field to advance a field of research. Research teams often consist of an independent investigator with expertise in biomedical optics and basic science, as well as physicians with expertise in the pathogenesis and systemic effects of the disease being investigated. With a research team that carries expertise in multiple arenas, some translation barriers can be avoided and research can often advance at a quicker pace. Such an interdisciplinary team allows members to train each other on technology issues, including the advantages and limitations of the technology, on disease pathophysiology, local and systemic disease effects, diagnoses, and treatments. Interdisciplinary teams such as these have been established and supported through the Network for Translational Research in Optical Imaging (NTROI) and through other NIH centers that bring together physicians and biomedical optics investigators.

4 Bench Work Poised for Clinical Translation

4.1 Molecular Imaging

The clinical utility of OCT would be greatly enhanced if it provided contrast to specific biomolecules. This capability, known as molecular imaging, has become a major emphasis in many areas of biomedical imaging.[170] Molecular imaging strategies can be divided into two broad classes: using exogenous contrast agents that are introduced into the body, which bind specifically to the biomolecules of interest (molecular contrast imaging); or direct imaging of the endogenous biomolecules (endogenous molecular imaging). The ability to design contrast agents for use with a variety of optical techniques makes molecular contrast imaging extremely attractive in spite of difficulties such as contrast agent toxicity, *in-vivo* agent transport and clearance, and specificity to the molecular target. In comparison, direct endogenous molecular imaging is not complicated by the introduction of outside agents, but is limited to the spectroscopic data obtained by directly querying the molecule.

4.1.1 Contrast agents

Contrast agents currently under development for OCT span a range of sizes and include single-molecule dyes, nanoparticles, and microspheres.[171] While many of these experimental agents are not yet approved for human use, most incorporate established nontoxic materials, such as gold or iron oxide. Although traditional fluorescent and bioluminescent probes do not emit coherent light, and thus provide no contrast with OCT, other agents that exhibit large optical scattering or absorption cross sections can be used to provide positive or negative contrast enhancement, respectively.

Similar to ultrasound contrast agents,[172] submicron particles and microspheres (>200 nm) are typically introduced into the blood pool or lymphatic system, where they remain until cleared via the reticuloendothelial system. Because arterial OCT imaging is well established,[63] targets of particular interest include inflammation (e.g., via phagocytosis by active macrophages) and angiogenesis (e.g., targeted via the integrin $\alpha_v\beta_3$ receptor) for identifying disease sites such as atherosclerotic plaques.[173] Liquid-core protein microspheres have been modified for OCT imaging by incorporating gold, carbon, and melanin nanoparticles into their shells to increase optical scattering.[88] These provide positive contrast in OCT and have been demonstrated in a mouse liver after injection in the tail vein.[88] In a related study, an RGD tripeptide was attached to the surface of protein microspheres via electrostatic layer-by-layer adhesion, and specificity to human colon tumor cells was demonstrated *in vitro*.[174] Another promising class of contrast agents includes silica-core gold-shelled particles, known as nanoshells, which exploit the surface-plasmon resonance property of gold.[175] Nanoshells 340 nm in diameter exhibit large backscattering efficiencies, which provide significant OCT contrast in tissue phantoms at concentrations near 10^9/mL.[176]

Smaller nanoparticles and molecules (<100 nm) have increased capacity to extravasate and thereby access tissue targets outside of the vasculature.[177] Fundamentally, the OCT attenuation due to these smaller contrast agents is dominated by absorption, not scattering. This is beneficial for photothermal therapy, where heat generated by light absorption kills targeted cells using light intensities significantly greater than those used for OCT imaging. This concept was demonstrated using nanoshells having an optical absorption peak at 820 nm. The nanoshells have been targeted to human breast cancer cells *in vitro* using an anti-HER2 antibody, and have also been shown to decrease tumor load in mice *in vivo*.[178]

Other types of gold plasmon-resonant structures have been investigated for imaging and therapy. Nanocages, which consist of 37-nm hollowed-out gold cubes, have been detected in tissue phantoms at 1-nM concentrations using OCT, and have also been coated with anti-HER2 antibodies for targeted imaging *in vitro*.[179] Nanorods of gold (15×45 nm in size) also provide absorption-based OCT contrast, and have been detected in 2% intralipid tissue phantoms at 30 ppm using an albedo-based detection algorithm.[180] Gold nanorods have also been used in photothermal therapy applications, and have been targeted to malignant cell lines using anti-EGFR antibodies.[181]

4.1.2 Spectroscopic contrast

Spectroscopic OCT signal analysis was first demonstrated for detection of optical absorption by melanin in an African frog tadpole,[182] and more recently has been applied to the assessment of blood oxygen saturation.[183] It is also possible to use endogenous spectroscopic OCT signals to determine the size and density of scatterers using Mie theory.[184] One promising application is nuclear size measurement for the detection of dysplastic changes in the esophagus, as demonstrated using angle-resolved low-coherence interferometry, a related technique.[133] Also, spectroscopic contrast and associated algorithms are required to augment traditional OCT scatterer siz-
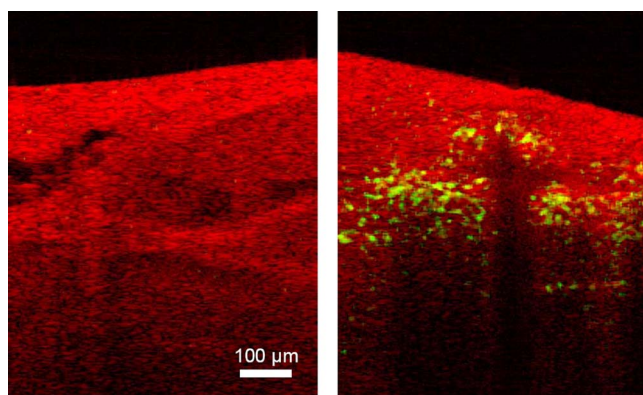
Fig. 9 Magnetomotive OCT images of freshly excised carcinogen-induced rat mammary tumor. Red displays the standard OCT image and green indicates magnetomotion. The left image is of control tumor tissue without nanoparticles. The right image is of tumor after injection with iron-oxide nanoparticles. Nanoparticles courtesy of Wuang and Pack (University of Illinois at Urbana-Champaign), images by Oldenburg and Boppart.

ing methods that are affected by multiple scatterers and variations in their size and density.[185] To this end, the spectroscopic OCT scattering and absorption signals, which are inherently coupled, may be separated using least-squares computational methods.[186]

Spectroscopic OCT has also been extensively explored for molecular imaging using contrast agents with well-characterized absorption or scattering signatures. Near-infrared dyes, including the FDA-approved agent indocyanine green,[95] have been used to provide absorption in specific spectral regions of interest.[93] A related principle is utilized for the detection of plasmon-resonant nanoparticles, which have a tunable absorption band that is ideally designed to absorb in a spectral region that is off-center with respect to the incident light.[187] This principle could potentially be used to track photodynamic therapy dyes during treatment, a concept that was recently demonstrated in tissue phantoms.[188]

4.1.3 Magnetomotive agents

Magnetic iron oxide nanoparticles are used as magnetic resonance imaging (MRI) contrast agents in humans, and are clinically useful for the detection of metastatic lymph nodes.[189] These nanoparticles may also be detected optically with high spatial resolution by perturbing them with an externally applied magnetic field gradient. The resulting nanometer-scale displacements (magnetomotion) give rise to light scattering changes observable with OCT (Fig. 9).[90] Magnetomotive OCT benefits from background rejection that is possible because of the correlation between scattering changes and field excitation. These techniques have been used to differentiate magnetically labeled from nonlabeled cells within 3-D scaffolds,[90] and to detect nanoparticles inside a living *Xenopus laevis* African frog tadpole[190] using a magnetic field modulated at 10 Hz. Because smaller imaging volumes are used in OCT than in MRI, the electromagnets are more compact and portable. Erythrocyte magnetomotion has also been detected in extracted blood using Doppler analysis of OCT signals, yielding a potential application to blood flow imaging.[191]

The ability to label magnetic iron oxide agents with antibodies or proteins to target diseased cells is an active area of interest.[192] Passive uptake models are also promising for targeting disease, such as exclusion by lymph node metastases[189] and endocytosis by macrophages in atherosclerotic plaques.[193] Coupling whole-body MRI or ultrasound imaging[194] with high-resolution magnetomotive OCT may become a powerful new tool for drug development for molecular imaging of nanoparticle uptake. Magnetic iron oxides also have potential therapeutic applications using hyperthermic therapy techniques, where magnetic fields are modulated at high frequencies ($>$100 kHz) to induce local heating.[195]

4.1.4 Pump probe and Raman

Molecular specificity may also be achieved using multiple light pulses or spectral wavelengths to probe the electronic or vibrational states of specific molecules. Coupling these techniques with interferometric imaging further increases the signal-to-noise ratio of such imaging. In pump-probe OCT, a pump pulse tuned to an electronic transition places a molecule into an excited state. A probe pulse monitors either the population transferred into the excited state, or its transient relaxation to an intermediate or ground state, which can be accomplished by several different methods.[196] In one study, the transient absorption of methylene blue dye was imaged using differential measurement of the OCT signal.[91] In another, the plant protein *phytochrome A*, which exhibits a switchable absorption maximum, was imaged using a two-color pump-probe method.[94] A technique not requiring two colors (and thus two light sources) has been implemented by monitoring ground-state recovery with a probe at the same wavelength as the pump.[197] Using this method, chromophores have been imaged within zebra fish, and differentiation of multiple chromophores such as hemoglobin and dyes has been demonstrated.[197]

Another promising technique for imaging endogenous molecules is coherent anti-Stokes Raman scattering (CARS). This is a four-wave mixing technique where three incident photons (two pump and one probe) mix to produce a fourth anti-Stokes photon. The anti-Stokes response is resonant if the pump/probe energy difference is equal to the vibrational energy level spacing. Thus, CARS measures molecules based on their vibrational bands, providing vibrational contrast in microscopy experiments.[198] Because CARS is a coherent process, it can be used for interferometric depth-resolved imaging, a technique known as nonlinear interferometric vibrational imaging (NIVI).[89] An important benefit of interferometric CARS is the ability to separate resonant and nonresonant signals, resulting in high molecular specificity.[199,200] To date, specificity to C-H vibrations in lipids has been demonstrated using *in-vitro* cell models[201] and in thicker constructs such as lipid-rich tissues.[86]

Although significant development will be necessary prior to translation of these techniques into the clinic, they exhibit great promise for noninvasive, endogenous molecular imaging.

4.2 Computational Techniques

Ongoing improvements to the instrumentation and signal processing used for OCT imaging continue to enhance acquisi-

tion speed and image fidelity. To maximize clinical utility, OCT instruments will need to provide real-time[202–213] imagery of 2-D slices and 3-D volumes. SD-OCT[214–219] has greatly increased the quality and acquisition speed of OCT images by increasing the signal-to-noise ratio[220–222] of acquired data. Swept-source imaging[223–227] greatly simplifies OCT instrumentation by scanning the wavelength of a rapidly tunable laser rather than using a broadband source such as a mode-locked laser or superluminescent diode. Recent advances such as Fourier-domain mode locking[228,229] are able to scan the wavelength hundreds of thousands of times per second, potentially providing video-rate imaging of 3-D volumes. A new method to scan the wavelength millions of times per second[230] has been demonstrated by sweeping the wavelength of every pulse produced by a supercontinuum laser source. With sufficient source power, this technique has the potential to sample billions of volume elements per second.

Such rapid data acquisition will require very fast signal processing to compute images from the data. Digital signal processing (DSP) has been incorporated into some OCT instrumentation to provide this capability.[231–234] Although analog electronics can be used for envelope detection to display structural images, Doppler OCT, one of the most important DSP applications in early OCT imaging,[235–237] requires phase-resolved imaging to capture flow-dependent time-varying phase data. With the advent of SD and SS-OCT, methods that require Fourier data analysis, DSP has become essential to modern OCT imaging. The well-demonstrated advantages of these methods over time-domain OCT will likely result in universal adoption of DSP techniques in OCT instruments. Finally, DSP-enabled 3-D computer graphics visualization[238–242] can be employed to allow dynamic visualization of tissues along arbitrary surfaces and planes, not just those that are biopsied and sectioned.

Computed imaging methods similar to those employed in x-ray computed tomography and magnetic resonance imaging are being increasingly employed for OCT to overcome OCT instrument limitations. As in conventional microscopy, OCT systems typically use objective lenses to focus light at a fixed depth in the tissue, causing features outside the focal volume to be poorly resolved. However, unlike traditional microscopy, OCT measures phase-resolved signals that can be used[243] to computationally image the out-of-focus features. This technique, called Interferometric Synthetic Aperture Microscopy[244] (ISAM), allows the out-of-focus features to be inferred from the phase information without scanning the focus. It can be implemented for both low and high[245] numerical aperture OCT imaging, rotationally scanned catheters used for endoscopy,[246] and full-field illumination microscopes.[247]

4.3 *Source Development*

The performance of OCT systems has been dramatically improved over the last decade by technological light source advances, and future enhancements in acquisition speed and imaging resolution are on the horizon. The axial resolution in an OCT image is inversely proportional to the bandwidth of the light source, and the sensitivity is proportional to the optical power. Thus, broadband light sources with high optical power are required for OCT imaging.[248] Additionally, optimal OCT imaging wavelengths are in the near-infrared spectral region

at approximately 700 to 1500 nm, where there is minimal light absorption by biological tissues. Simple broadband sources such as tungsten or xenon lamps can be used to provide hundreds of nanometers of bandwidth, but are limited by low fluence that significantly limits the single-mode coupled power needed for interferometric imaging.[249,250] Pulsed lamp sources can, however, be used with full-field OCT systems to obtain ultrahigh resolution, real-time images.[251] Other spontaneous emission sources such as semiconductor optical amplifiers (SOAs),[219] superluminescent diodes,[252,253] and diode-pumped NIR gain media[254,255] are typically inexpensive and commercially available.

Ultrashort pulse mode-locked lasers are also widely used for OCT imaging. The most common is the Ti:sapphire laser, centered near 800 nm with bandwidths ranging from 150 to 350 nm,[256,257] with turnkey commercial sources available.[258] Future sources under investigation include low-cost mode-locked Ti:sapphire lasers with lower pump power requirements,[259] or lasers that can be directly diode pumped.[260,261] Because ultrashort pulses have extremely high peak powers, they cause nonlinear interactions such as self-phase modulation, thereby broadening the optical bandwidth (also known as supercontinuum generation). This is extremely convenient for enhancing the resolution of OCT systems, since supercontinua, which are typically obtained by focusing laser light into a single-mode silica fiber, can be generated in the same fiber used for beam delivery.[202,206,261–266] Microstructured fibers, also known as photonic crystal fibers, are designed with anomalous dispersion characteristics that increase the interaction length of light pulses for more efficient supercontinuum generation,[267] and have been used for *in-vivo* OCT imaging,[268] producing bandwidths over 300 nm and nominally tens of milliwatts of output power.[269–274] Several nonlinear processes involved in this supercontinuum generation, however, may exhibit greater noise in comparison to the self-phase modulation in silica fibers.[268,274]

Fourier-domain OCT systems may also employ frequency-swept light sources,[223,225] which have sensitivity advantages over time-domain OCT systems,[224,275] and enable high-speed imaging that reduces motion artifacts during *in-vivo* imaging.[276] Most swept-source systems are based on SOAs operating with a center wavelength near 1300 nm,[227,277–279] although shorter wavelengths have recently become available.[280–282] Fourier-domain mode-locking sources synchronize the wavelength sweep with the laser cavity roundtrip time, permitting exceptionally high sweep rates (>200 kHz) for real-time imaging.[228,229]

5 Conclusion

This work has given an overview of the development of OCT, the current state of research and commercial development, and the future of clinical OCT imaging. The development of advanced OCT source, beam delivery, and detection technologies has driven investigations into a wide array of clinical applications in the fields of ophthalmology, cardiology, and oncology, among many others. As new technological advances are made to enhance contrast, provide molecular sensitivity, enhance image features, and speed image acquisition, new OCT applications will certainly be enabled. The future of OCT will continue to benefit from and be strengthened by the

translational research of moving technology from the bench to the bedside, and back again.

Acknowledgments

References

1. D. Huang, E. A. Swanson, C. P. Lin, J. S. Schuman, W. G. Stinson, W. Chang, M. R. Hee, T. Flotte, K. Gregory, C. A. Puliafito, and J. G. Fujimoto, "Optical coherence tomography," *Science* **254**(5035) 1178–1181 (1991).
2. M. Brezinski, *Optical Coherence Tomography: Principles and Applications*, Academic Press, London (2006).
3. B. E. Bouma and G. J. Tearney, *Handbook of Optical Coherence Tomography*, Informa Healthcare, New York (2001).
4. K. Takada, I. Yokohama, K. Chida, and J. Noda, "New measurement system for fault location in optical waveguide devices based on an interferometric technique," *Appl. Opt.* **26**(9), 1603–1606 (1987).
5. R. C. Youngquist, S. Carr, and D. E. N. Davies, "Optical coherence-domain reflectometry: a new optical evaluation technique," *Opt. Lett.* **12**(3), 158–160 (1987).
6. A. F. Fercher, K. Mengedoht, and W. Werner, "Eye-length measurement by interferometry with partially coherent light," *Opt. Lett.* **13**(3), 186–188 (1988).
7. "Carl Zeiss Meditec Announces Installation of 6,000th Stratus OCT," Carl Zeiss Meditec, Inc., Dublin, CA (2006).
8. M. Walz, "Hot technologies for 2007: OCT: imaging of the future," *R&D Mag.*, **6**(12) (2006).
9. R. A. Costa, M. Skaf, L. A. S. Melo, D. Calucci, J. A. Cardillo, J. C. Castro, D. Huang, and M. Wojtkowski, "Retinal assessment using optical coherence tomography," *Prog. Retin Eye Res.* **25**(3), 325–353 (2006).
10. M. R. Dogra, A. Gupta, and V. Gupta, *Atlas of Optical Coherence Tomography of Macular Diseases*, Taylor & Francis, New York (2004).
11. M. R. Hee, C. A. Puliafito, C. Wong, J. S. Duker, E. Reichel, B. Rutledge, J. S. Schuman, E. A. Swanson, and J. G. Fujimoto, "Quantitative assessment of macular edema with optical coherence tomography," *Arch. Ophthalmol. (Chicago)* **113**(8), 1019–1029 (1995).
12. J. S. Schuman, C. A. Puliafito, and J. G. Fujimoto, *Optical Coherence Tomography of Ocular Diseases*, Slack, Inc., Thorofare, NJ (2004).
13. L. Alexander and W. Choate, "Optical coherence tomography: rewriting the standard of care in diagnosis, management and interventional assessment," *Rev. Optometry* **141**(9), 1CE–8CE (2004).
14. E. Uchino, A. Uemura, and N. Ohba, "Initial stages of posterior vitreous detachment in healthy eyes of older persons evaluated by optical coherence tomography," *Arch. Ophthalmol. (Chicago)* **119**(10), 1475–1479 (2001).
15. M. Altaweel and M. Ip, "Macular hole: improved understanding of pathogenesis, staging, and management based on optical coherence tomography," *Semin Ophthalmol.* **18**(2), 58–66 (2003).
16. A. Gaudric, B. Haouchine, P. Massin, M. Paques, P. Blain, and A. Erginay, "Macular hole formation: new data provided by optical coherence tomography," *Arch. Ophthalmol. (Chicago)* **117**(6), 744–751 (1999).
17. M. R. Hee, C. A. Puliafito, C. Wong, J. S. Duker, E. Reichel, J. S. Schuman, E. A. Swanson, and J. G. Fujimoto, "Optical coherence tomography of macular holes," *Ophthalmology* **102**(5), 748–756 (1995).
18. C. A. Puliafito, M. R. Hee, C. P. Lin, E. Reichel, J. S. Schuman, J. S. Duker, J. A. Izatt, E. A. Swanson, and J. G. Fujimoto, "Imaging of macular diseases with optical coherence tomography," *Ophthalmology* **102**(2), 217–229 (1995).
19. M. N. Apostolopoulos, C. N. Koutsandrea, M. N. Moschos, D. A. Alonistiotis, A. E. Papaspyrou, J. A. Mallias, T. E. Kyriaki, P. G. Theodossiadis, and G. P. Theodossiadis, "Evaluation of successful macular hole surgery by optical coherence tomography and multifocal electroretinography," *Am. J. Ophthalmol.* **134**(5), 667–674 (2002).
20. J. M. Jumper, R. P. Gallemore, B. W. McCuen, and C. A. Toth, "Features of macular hole closure in the early postoperative period using optical coherence tomography," *Retina* **20**(3), 232–237 (2000).
21. H. Sato, R. Kawasaki, and H. Yamashita, "Observation of idiopathic full-thickness macular hole closure in early postoperative period as evaluated by optical coherence tomography," *Am. J. Ophthalmol.* **136**(1), 185–187 (2003).
22. R. J. Antcliff, M. R. Stanford, D. S. Chauhan, E. M. Graham, D. J. Spalton, J. S. Shilling, T. J. ffytche, and J. Marshall, "Comparison between optical coherence tomography and fundus fluorescein angiography for the detection of cystoid macular edema in patients with uveitis," *Ophthalmology* **107**(3), 593–599 (2000).
23. M. R. Hee, C. A. Puliafito, J. S. Duker, E. Reichel, J. G. Coker, J. R. Wilkins, J. S. Schuman, E. A. Swanson, and J. G. Fujimoto, "Topography of diabetic macular edema with optical coherence tomography," *Ophthalmology* **105**(2), 360–370 (1998).
24. P. Massin, C. Allouch, B. Haouchine, F. Metge, M. Paques, L. Tangui, A. Erginay, and A. Gaudric, "Optical coherence tomography of idiopathic macular epiretinal membranes before and after surgery," *Am. J. Ophthalmol.* **130**(6), 732–739 (2000).
25. T. Otani, S. Kishi, and Y. Maruyama, "Patterns of diabetic macular edema with optical coherence tomography," *Am. J. Ophthalmol.* **127**(6), 688–693 (1999).
26. M. R. Hee, C. R. Baumal, C. A. Puliafito, J. S. Duker, E. Reichel, J. R. Wilkins, J. G. Coker, J. S. Schuman, E. A. Swanson, and J. G. Fujimoto, "Optical coherence tomography of age-related macular degeneration and choroidal neovascularization," *Ophthalmology* **103**(8), 1260–1270 (1996).
27. F. A. Medeiros, L. M. Zangwill, C. Bowd, R. M. Vessani, R. Susanna, and R. N. Weinreb, "Evaluation of retinal nerve fiber layer, optic nerve head, and macular thickness measurements for glaucoma detection using optical coherence tomography," *Am. J. Ophthalmol.* **139**(1), 44–55 (2005).
28. M. Mujat, R. C. Chan, B. Cense, B. H. Park, C. Joo, T. Akkin, T. C. Chen, and J. F. de Boer, "Retinal nerve fiber layer thickness map determined from optical coherence tomography images," *Opt. Express* **13**(23), 9480–9491 (2005).
29. E. Z. Blumenthal, J. M. Williams, R. N. Weinreb, C. A. Girkin, C. C. Berry, and L. M. Zangwill, "Reproducibility of nerve fiber layer thickness measurements by use of optical coherence tomography," *Ophthalmology* **107**(12), 2278–2282 (2000).
30. D. L. Budenz, R. T. Chang, X. Huang, R. W. Knighton, and J. M. Tielsch, "Reproducibility of retinal nerve fiber thickness measurements using the Stratus OCT in normal and glaucomatous eyes," *Invest. Ophthalmol. Visual Sci.* **46**(7), 2440–2443 (2005).
31. P. Carpineto, M. Ciancaglini, E. Zuppardi, G. Falconio, E. Doronzo, and L. Mastropasqua, "Reliability of nerve fiber layer thickness measurements using optical coherence tomography in normal and glaucomatous eyes," *Ophthalmology* **110**(1), 190–195 (2003).
32. L. A. Paunescu, J. S. Schuman, L. L. Price, P. C. Stark, S. Beaton, H. Ishikawa, G. Wollstein, and J. G. Fujimoto, "Reproducibility of nerve fiber thickness, macular thickness, and optic nerve head measurements using StratusOCT," *Invest. Ophthalmol. Visual Sci.* **45**(6), 1716–1724 (2004).
33. G. Wollstein, J. S. Schuman, L. L. Price, A. Aydin, P. C. Stark, E. Hertzmark, E. Lai, H. Ishikawa, C. Mattox, J. G. Fujimoto, and L. A.

Paunescu, "Optical coherence tomography longitudinal evaluation of retinal nerve fiber layer thickness in glaucoma," *Arch. Ophthalmol. (Chicago)* **123**(4), 464–470 (2005).

34. C. K. S. Leung, W. H. Yung, A. C. K. Ng, J. Woo, M. K. Tsang, and K. K. Tse, "Evaluation of scanning resolution on retinal nerve fiber layer measurement using optical coherence tomography in normal and glaucomatous eyes," *J. Glaucoma* **13**(6), 479–485 (2004).

35. J. S. Schuman, M. R. Hee, C. A. Puliafito, C. Wong, T. Pedut-Kloizman, C. P. Lin, E. Hertzmark, J. A. Izatt, E. A. Swanson, and J. G. Fujimoto, "Quantification of nerve fiber layer thickness in normal and glaucomatous eyes using optical coherence tomography: A pilot study," *Arch. Ophthalmol. (Chicago)* **113**(5), 586–596 (1995).

36. C. A. Sánchez-Galeana, C. Bowd, L. M. Zangwill, P. A. Sample, and R. N. Weinreb, "Short-wavelength automated perimetry results are correlated with optical coherence tomography retinal nerve fiber layer thickness measurements in glaucomatous eyes," *Ophthalmology* **111**(10), 1866–1872 (2004).

37. D. Thomas and G. Duguid, "Optical coherence tomography—a review of the principles and contemporary uses in retinal investigation," *Eye* **18**(6), 561–570 (2004).

38. M. Pircher, E. Götzinger, R. Leitgeb, A. F. Fercher, and C. K. Hitzenberger, "Measurement and imaging of water concentration in human cornea with differential absorption optical coherence tomography," *Opt. Express* **11**(18), 2190–2197 (2003).

39. R. A. Costa, L. Scapucin, N. S. Moraes, D. Calucci, L. A. Melo, J. A. Cardillo, and M. E. Farah, "Indocyanine green-mediated photothrombosis as a new technique of treatment for persistent central serous chorioretinopathy," *Curr. Eye Res.* **25**(5), 287–297 (2002).

40. P. A. Campochiaro, "Reduction of diabetic macular edema by oral administration of the kinase inhibitor PKC412," *Invest. Ophthalmol. Visual Sci.* **45**(3), 922–931 (2004).

41. S. Michels, P. J. Rosenfeld, C. A. Puliafito, E. N. Marcus, and A. S. Venkatraman, "Systemic bevacizumab (avastin) therapy for neovascular age-related macular degeneration: Twelve-week results of an uncontrolled open-label clinical study," *Ophthalmology* **112**(6), 1035–1047 (2005).

42. J. A. Cardillo, L. A. S. Melo, R. A. Costa, M. Skaf, R. Belfort, A. A. Souza-Filho, M. E. Farah, and B. D. Kuppermann, "Comparison of intravitreal versus posterior sub-tenon's capsule injection of triamcinolone acetonide for diffuse diabetic macular edema," *Ophthalmology* **112**(9), 1557–1563 (2005).

43. M. A. Bonini-Filho, R. Jorge, J. C. Barbosa, D. Calucci, J. A. Cardillo, and R. A. Costa, "Intravitreal injection versus sub-tenon's infusion of triamcinolone acetonide for refractory diabetic macular edema: A randomized clinical trial," *Invest. Ophthalmol. Visual Sci.* **46**(10), 3845–3849 (2005).

44. N. Eter, and R. F. Spaide, "Comparison of fluorescein angiography and optical coherence tomography for patients with choroidal neovascularization after photodynamic therapy," *Retina* **25**(6), 691–696 (2005).

45. A. Salinas-Alamán, A. García-Layana, M. J. Maldonado, C. Sainz-Gómez, and A. Alvárez-Vidal, "Using optical coherence tomography to monitor photodynamic therapy in age related macular degeneration," *Am. J. Ophthalmol.* **140**(1), 23–28 (2005).

46. J. Sahni, P. Stanga, D. Wong, and S. Harding, "Optical coherence tomography in photodynamic therapy for subfoveal choroidal neovascularisation secondary to age related macular degeneration: a cross sectional study," *Br. J. Ophthalmol.* **89**(3), 316–320 (2005).

47. C. K. Hitzenberger, P. Trost, P. W. Lo, and Q. Zhou, "Three-dimensional imaging of the human retina by high-speed optical coherence tomography," *Opt. Express* **11**(21), 2753–2761 (2003).

48. M. Pircher, E. Götzinger, O. Findl, S. Michels, W. Geitzenauer, C. Leydolt, U. Schmidt-Erfurth, and C. K. Hitzenberger, "Human macula investigated in vivo with polarization-sensitive optical coherence tomography," *Invest. Ophthalmol. Visual Sci.* **47**(12), 5487–5495 (2006).

49. E. Götzinger, M. Pircher, M. Sticker, A. F. Fercher, and C. K. Hitzenberger, "Measurement and imaging of birefringent properties of the human cornea with phase-resolved, polarization-sensitive optical coherence tomography," *J. Biomed. Opt.* **9**(1), 94–102 (2004).

50. Y. Zhang, J. Rha, R. S. Jonnal, and D. T. Miller, "Adaptive optics parallel spectral domain optical coherence tomography for imaging the living retina," *Opt. Express* **13**(12), 4792–4811 (2005).

51. R. J. Zawadzki, S. M. Jones, S. S. Olivier, M. Zhao, B. A. Bower, J. A. Izatt, S. Choi, S. Laut, and J. S. Werner, "Adaptive-optics optical coherence tomography for high-resolution and high-speed 3D retinal in vivo imaging," *Opt. Express* **13**(21), 8532–8546 (2005).

52. K. Bizheva, R. Pflug, B. Hermann, B. Povazay, H. Sattmann, P. Qiu, E. Anger, H. Reitsamer, S. Popov, J. R. Taylor, A. Unterhuber, P. Ahnelt, and W. Drexler, "Optophysiology: Depth-resolved probing of retinal physiology with functional ultrahigh-resolution optical coherence tomography," *Proc. Natl. Acad. Sci. U.S.A.* **103**(13), 5066–5071 (2006).

53. B. E. Bouma and G. J. Tearney, "Clinical imaging with optical coherence tomography," *Acad. Radiol.* **9**(8), 942–953 (2002).

54. B. E. Bouma, G. J. Tearney, H. Yabushita, M. Shishkov, C. R. Kauffman, D. DeJoseph Gauthier, B. D. MacNeill, S. L. Houser, H. T. Aretz, E. F. Halpern, and I. K. Jang, "Evaluation of intracoronary stenting by intravascular optical coherence tomography," *Heart* **89**(3), 317–320 (2003).

55. M. E. Brezinski, G. J. Tearney, B. E. Bouma, J. A. Izatt, M. R. Hee, E. A. Swanson, J. F. Southern, and J. G. Fujimoto, "Optical coherence tomography for optical biopsy: Properties and demonstration of vascular pathology," *Circulation* **93**(6), 1206–1213 (1996).

56. M. E. Brezinski, G. J. Tearney, B. E. Bouma, S. A. Boppart, M. R. Hee, E. A. Swanson, J. F. Southern, and J. G. Fujimoto, "Imaging of coronary artery microstructure (in vitro) with optical coherence tomography," *Am. J. Cardiol.* **77**(1), 92–93 (1996).

57. M. E. Brezinski, G. J. Tearney, N. J. Weissman, S. A. Boppart, B. E. Bouma, M. R. Hee, A. E. Weyman, E. A. Swanson, J. F. Southern, and J. G. Fujimoto, "Assessing atherosclerotic plaque morphology: comparison of optical coherence tomography and high frequency intravascular ultrasound," *Heart* **77**(5), 397–403 (1997).

58. A. H. Chau, R. C. Chan, M. Shishkov, B. MacNeill, N. Iftimia, G. J. Tearney, R. D. Kamm, B. E. Bouma, and M. R. Kaazempur-Mofrad, "Mechanical analysis of atherosclerotic plaques based on optical coherence tomography," *Ann. Biomed. Eng.* **32**(11), 1494–1503 (2004).

59. J. G. Fujimoto, S. A. Boppart, G. J. Tearney, B. E. Bouma, C. Pitris, and M. E. Brezinski, "High resolution in vivo intra-arterial imaging with optical coherence tomography," *Heart* **82**(2), 128–133 (1999).

60. M. Gupta, A. M. Rollins, J. A. Izatt, and I. R. Efimov, "Imaging of the atrioventricular node using optical coherence tomography," *J. Cardiovasc. Electrophysiol.* **13**(1), 95 (2002).

61. I. K. Jang, G. Tearney, and B. Bouma, "Visualization of tissue prolapse between coronary stent struts by optical coherence tomography: Comparison with intravascular ultrasound," *Circulation* **104**(22), 2754 (2001).

62. I. K. Jang, B. E. Bouma, D. H. Kang, S. J. Park, S. W. Park, K. B. Seung, K. B. Choi, M. Shishkov, K. Schlendorf, E. Pomerantsev, S. L. Houser, H. T. Aretz, and G. J. Tearney, "Visualization of coronary atherosclerotic plaques in patients using optical coherence tomography: comparison with intravascular ultrasound," *J. Am. Coll. Cardiol.* **39**(4), 604–609 (2002).

63. I. K. Jang, G. J. Tearney, B. MacNeill, M. Takano, F. Moselewski, N. Iftima, M. Shishkov, S. Houser, H. T. Aretz, E. F. Halpern, and B. E. Bouma, "In vivo characterization of coronary atherosclerotic plaque by use of optical coherence tomography," *Circulation* **111**(12), 1551–1555 (2005).

64. B. D. MacNeill, I. K. Jang, B. E. Bouma, N. Iftimia, M. Takano, H. Yabushita, M. Shishkov, C. R. Kauffman, S. L. Houser, H. T. Aretz, D. DeJoseph, E. F. Halpern, and G. J. Tearney, "Focal and multi-focal plaque macrophage distributions in patients with acute and stable presentations of coronary artery disease," *J. Am. Coll. Cardiol.* **44**(5), 972–979 (2004).

65. G. J. Tearney, M. E. Brezinski, S. A. Boppart, B. E. Bouma, N. Weissman, J. F. Southern, E. A. Swanson, and J. G. Fujimoto, "Catheter-based optical imaging of a human coronary artery," *Circulation* **94**(11), 3013 (1996).

66. G. J. Tearney, M. E. Brezinski, B. E. Bouma, S. A. Boppart, C. Pitris, J. F. Southern, and J. G. Fujimoto, "In vivo endoscopic optical biopsy with optical coherence tomography," *Science* **276**(5321), 2037–2039 (1997).

67. G. J. Tearney and B. E. Bouma, Method and apparatus for determination of atherosclerotic plaque type by measurement of tissue optical properties, U.S. Patent Application 20030028100 (2003).

68. G. J. Tearney, H. Yabushita, S. L. Houser, H. T. Aretz, I. K. Jang, K. H. Schlendorf, C. R. Kauffman, M. Shishkov, E. F. Halpern, and B. E. Bouma, "Quantification of macrophage content in atherosclerotic plaques by optical coherence tomography," *Circulation* **107**(1), 113–119 (2003).

69. H. Yabushita, B. E. Bouma, S. L. Houser, H. T. Aretz, I. K. Jang, K. H. Schlendorf, C. R. Kauffman, M. Shishkov, D. H. Kang, E. F. Halpern, and G. J. Tearney, "Characterization of human atherosclerosis by optical coherence tomography," *Circulation* **106**(13), 1640–1645 (2002).

70. T. M. Yelbuz, M. A. Choma, L. Thrane, M. L. Kirby, and J. A. Izatt, "Optical coherence tomography: a new high-resolution imaging technology to study cardiac development in chick embryos," *Circulation* **106**(22), 2771–2774 (2002).

71. W. Luo, D. L. Marks, T. S. Ralston, and S. A. Boppart, "Three-dimensional optical coherence tomography of the embryonic murine cardiovascular system," *J. Biomed. Opt.* **11**(2), 021014 (2006).

72. A. F. Zuluaga and B. E. Bouma, Multi-channel optical coupler for spinning catheter, U.S. Patent No. 6,895,137 (2005).

73. D. Yelin, B. E. Bouma, N. Iftimia, and G. J. Tearney, "Three-dimensional spectrally encoded imaging," *Opt. Lett.* **28**(23), 2321–2323 (2003).

74. "Heart disease and stroke statistics—2005 update," American Heart Association, Dallas, Texas (2005).

75. G. J. Tearney, I. K. Jang, and B. E. Bouma, "Optical coherence tomography for imaging the vulnerable plaque," *J. Biomed. Opt.* **11**(2), 021002 (2006).

76. B. D. MacNeill, B. E. Bouma, H. Yabushita, I. K. Jang, and G. J. Tearney, "Intravascular optical coherence tomography: cellular imaging," *J. Nucl. Cardiol.* **12**(4), 460–465 (2005).

77. T. Kume, T. Akasaka, T. Kawamoto, N. Watanabe, E. Toyota, Y. Neishi, R. Sukmawan, Y. Sadahira, and K. Yoshida, "Assessment of coronary intima-media thickness by optical coherence tomography: comparison with intravascular ultrasound," *Jpn. Circ. J.* **69**(8), 903–907 (2005).

78. T. Kume, T. Akasaka, T. Kawamoto, H. Okura, N. Watanabe, E. Toyota, Y. Neishi, R. Sukmawan, Y. Sadahira, and K. Yoshida, "Measurement of the thickness of the fibrous cap by optical coherence tomography," *Am. Heart J.* **152**(4), 755e1-755e4 (2006).

79. F. J. van der Meer, D. J. Faber, D. M. B. Sassoon, M. C. Aalders, G. Pasterkamp, and T. G. van Leeuwen, "Localized measurement of optical attenuation coefficients of atherosclerotic plaque constituents by quantitative optical coherence tomography," *IEEE Trans. Med. Imaging* **24**(10), 1369–1376 (2005).

80. F. J. van der Meer, D. J. Faber, J. Perrée, G. Pasterkamp, D. B. Sassoon, and T. G. van Leeuwen, "Quantitative optical coherence tomography of arterial wall components," *Lasers Med. Sci.* **20**(1), 45–51 (2005).

81. Y. Takeda and O. Katoh, "OCT-guided wiring technique for chronic total coronary occlusion," in *Optical Coherence Tomography in Cardiovascular Research*, E. Regar, T. G. van Leeuwen, and P. W. Serruys, Eds., pp. 183–190, Informa Healthcare, London (2007).

82. J. Tanigawa, O. Katoh, and C. Di Mario, "Chronic total occlusion: do we need intravascular imaging guidance?" in *Optical Coherence Tomography in Cardiovascular Research*, E. Regar, T. G. van Leeuwen, and P. W. Serruys, Eds., pp. 171–182, Informa Healthcare, London (2007).

83. T. Kume, T. Akasaka, T. Kawamoto, N. Watanabe, E. Toyota, R. Sukmawan, Y. Sadahira, and K. Yoshida, "Visualization of neointima formation by optical coherence tomography," *Intl. Heart J.* **46**(6), 1133–1136 (2005).

84. E. Regar, H. M. M. van Beusekom, W. J. van der Giessen, and P. W. Serruys, "Optical coherence tomography findings at 5-year follow-up after coronary stent implantation," *Circulation* **112**(23), e345–e346 (2005).

85. J. F. Surmely, Y. Takeda, T. Ito, and T. Suzuki, "Acute OCT findings after stenting," in *Optical Coherence Tomography in Cardiovascular Research*, E. Regar, T. G. van Leeuwen, and P. W. Serruys, Eds., pp. 153–160, Informa Healthcare, London(2007).

86. J. S. Bredfeldt, C. Vinegoni, D. L. Marks, and S. A. Boppart, "Molecularly sensitive optical coherence tomography," *Opt. Lett.* **30**(5), 495–497 (2005).

87. M. Lazebnik, D. L. Marks, K. Potgieter, R. Gillette, and S. A. Boppart, "Functional optical coherence tomography for detecting neural activity through scattering changes," *Opt. Lett.* **28**(14), 1218–1220 (2003).

88. T. M. Lee, A. L. Oldenburg, S. Sitafalwalla, D. L. Marks, W. Luo, F. J. J. Toublan, K. S. Suslick, and S. A. Boppart, "Engineered microsphere contrast agents for optical coherence tomography," *Opt. Lett.* **28**(17), 1546–1548 (2003).

89. D. L. Marks and S. A. Boppart, "Nonlinear interferometric vibrational imaging," *Phys. Rev. Lett.* **92**(12), 123905 (2004).

90. A. L. Oldenburg, J. R. Gunther, and S. A. Boppart, "Imaging magnetically labeled cells with magnetomotive optical coherence tomography," *Opt. Lett.* **30**(7), 747–749 (2005).

91. K. D. Rao, M. A. Choma, S. Yazdanfar, A. M. Rollins, and J. A. Izatt, "Molecular contrast in optical coherence tomography by use of a pump-probe technique," *Opt. Lett.* **28**(5), 340–342 (2003).

92. J. E. Roth, J. A. Izatt, and A. M. Rollins, Method and apparatus for polarization-sensitive optical coherence tomography, U.S. Patent Application 20020196446 (2002).

93. C. Xu, J. Ye, D. L. Marks, and S. A. Boppart, "Near-infrared dyes as contrast-enhancing agents for spectroscopic optical coherence tomography," *Opt. Lett.* **29**(14), 1647–1649 (2004).

94. C. Yang, M. A. Choma, L. E. Lamb, J. D. Simon, and J. A. Izatt, "Protein-based molecular contrast optical coherence tomography with phytochrome as the contrast agent," *Opt. Lett.* **29**(12), 1396–1398 (2004).

95. C. Yang, L. E. L. McGuckin, J. D. Simon, M. A. Choma, B. E. Applegate, and J. A. Izatt, "Spectral triangulation molecular contrast optical coherence tomography with indocyanine green as the contrast agent," *Opt. Lett.* **29**(17), 2016–2018 (2004).

96. C. Yang, "Molecular contrast optical coherence tomography: A review," *Photochem. Photobiol.* **81**(2), 215–237 (2005).

97. S. D. Giattina, B. K. Courtney, P. R. Herz, M. Harman, S. Shortkroff, D. L. Stamper, B. Liu, J. G. Fujimoto, and M. E. Brezinski, "Assessment of coronary plaque collagen with polarization sensitive optical coherence tomography (PS-OCT)," *Int. J. Cardiol.* **107**(3), 400–409 (2006).

98. W. C. Kuo, N. K. Chou, C. Chou, C. M. Lai, H. J. Huang, S. S. Wang, and J. J. Shyu, "Polarization-sensitive optical coherence tomography for imaging human atherosclerosis," *Appl. Opt.* **46**(13), 2520–2527 (2007).

99. A. I. Kholodnykh, I. Y. Petrova, M. Motamedi, and R. O. Esenaliev, "Accurate measurement of total attenuation coefficient of thin tissue with optical coherence tomography," *IEEE J. Sel. Top. Quantum Electron.* **9**(2), 210–221 (2003).

100. F. J. van der Meer, D. J. Faber, I. Çilesiz, M. J. C. Van Gemert, and T. G. van Leeuwen, "Temperature-dependent optical properties of individual vascular wall components measured by optical coherence tomography," *J. Biomed. Opt.* **11**(4), 041120 (2006).

101. J. Rogowska, N. A. Patel, J. G. Fujimoto, and M. E. Brezinski, "Optical coherence tomographic elastography technique for measuring deformation and strain of atherosclerotic tissues," *Heart* **90**(5), 556–562 (2004).

102. J. Rogowska, N. Patel, S. Plummer, and M. E. Brezinski, "Quantitative optical coherence tomographic elastography: method for assessing arterial mechanical properties," *Br. J. Radiol.* **79**(945), 707–711 (2006).

103. S. A. Boppart, W. Luo, D. L. Marks, and K. W. Singletary, "Optical coherence tomography: feasibility for basic research and image-guided surgery of breast cancer," *Breast Cancer Res. Treat.* **84**(2), 85–97 (2004).

104. A. M. Zysk and S. A. Boppart, "Computational methods for analysis of human breast tumor tissue in optical coherence tomography images," *J. Biomed. Opt.* **11**(5), 054015 (2006).

105. D. Cao, C. Lin, S. H. Woo, R. Vang, T. N. Tsangaris, and P. Argani, "Separate cavity margin sampling at the time of initial breast lumpectomy significantly reduces the need for reexcisions," *Am. J. Surg. Pathol.* **29**(12), 1625–1632 (2005).

106. F. T. Nguyen, A. M. Zysk, J. G. Kotynek, F. J. Bellafiore, K. M. Rowland, P. A. Johnson, E. J. Chaney, and S. A. Boppart, "Portable real-time optical coherence tomography system for intraoperative imaging and staging of breast cancer," *Proc. SPIE* **6430**, 64300H (2007).

107. W. Luo, F. T. Nguyen, A. M. Zysk, T. S. Ralston, J. Brockenbrough, D. L. Marks, A. L. Oldenburg, and S. A. Boppart, "Optical biopsy of lymph node morphology using optical coherence tomography," *Technol. Cancer Res. Treat.* **4**(5), 539–548 (2005).

108. N. V. Iftimia, B. E. Bouma, M. B. Pitman, B. Goldberg, J. Bressner, and G. J. Tearney, "A portable, low coherence interferometry based instrument for fine needle aspiration biopsy guidance," *Rev. Sci. Instrum.* **76**(6), 064301 (2005).

109. A. F. Zuluaga, M. Follen, I. Boiko, A. Malpica, and R. Richards-Kortum, "Optical coherence tomography: A pilot study of a new

imaging technique for noninvasive examination of cervical tissue," *Am. J. Obstet. Gynecol.* **193**(1), 83–88 (2005).

110. A. M. Zysk, S. G. Adie, J. J. Armstrong, M. S. Leigh, A. Paduch, D. D. Sampson, F. T. Nguyen, and S. A. Boppart, "Needle-based refractive index measurement using low-coherence interferometry," *Opt. Lett.* **32**(4), 385–387 (2007).

111. A. M. Zysk, D. L. Marks, D. Y. Liu, and S. A. Boppart, "Needle-based reflection refractometry of scattering samples using coherence-gated detection," *Opt. Express* **15**(8), 4787–4794 (2007).

112. P. R. Herz, Y. Chen, A. D. Aguirre, K. Schneider, P. Hsiung, J. G. Fujimoto, K. Madden, J. Schmitt, J. Goodnow, and C. Petersen, "Micromotor endoscope catheter for *in vivo*, ultrahigh-resolution optical coherence tomography," *Opt. Lett.* **29**(19), 2261–2263 (2004).

113. P. H. Tran, D. S. Mukai, M. Brenner, and Z. Chen, "*In vivo* endoscopic optical coherence tomography by use of a rotational microelectromechanical system probe," *Opt. Lett.* **29**(11), 1236–1238 (2004).

114. T. Xie, H. Xie, G. K. Fedder, and Y. Pan, "Endoscopic optical coherence tomography with a modified microelectromechanical systems mirror for detection of bladder cancers," *Appl. Opt.* **42**(31), 6422–6426 (2003).

115. A. G. Bibas, A. G. Podoleanu, R. G. Cucu, M. Bonmarin, G. M. Dobre, V. M. M. Ward, E. Odell, A. Boxer, M. J. Gleeson, and D. A. Jackson, "3-D optical coherence tomography of the laryngeal mucosa," *Clin. Otolaryngol.* **29**(6), 713–720 (2004).

116. W. B. Armstrong, J. M. Ridgway, D. E. Vokes, S. Guo, J. Perez, R. P. Jackson, M. Gu, J. Su, R. L. Crumley, T. Y. Shibuya, U. Mahmood, Z. Chen, and B. J. F. Wong, "Optical coherence tomography of laryngeal cancer," *Laryngoscope* **116**(7), 1107–1113 (2006).

117. B. J. F. Wong, R. P. Jackson, S. Guo, J. M. Ridgway, U. Mahmood, J. Su, T. Y. Shibuya, R. L. Crumley, M. Gu, W. B. Armstrong, and Z. Chen, "In vivo optical coherence tomography of the human larynx: normative and benign pathology in 82 patients," *Laryngoscope* **115**(11), 1904–1911 (2005).

118. K. Lüerβen, H. Lubatschowski, K. Ursinus, H. Gasse, R. Koch, and M. Ptok, "Optical coherence tomography in the diagnosis of vocal folds," *HNO* **54**(8), 611–615 (2006).

119. U. Mahmood, J. Ridgway, R. Jackson, S. Guo, J. Su, W. Armstrong, T. Shibuya, R. Crumley, Z. Chen, and B. Wong, "*In vivo* optical coherence tomography of the nasal mucosa," *Am. J. Rhinol.* **20**(2), 155–159 (2006).

120. J. M. Ridgway, W. B. Armstrong, S. Guo, U. Mahmood, J. Su, R. P. Jackson, T. Shibuya, R. L. Crumley, M. Gu, Z. Chen, and B. J. F. Wong, "In vivo optical coherence tomography of the human oral cavity and oropharynx," *Arch. Otolaryngol. Head Neck Surg.* **132**(10), 1074–1081 (2006).

121. S. Brand, J. M. Poneros, B. E. Bouma, G. J. Tearney, C. C. Compton, and N. S. Nishioka, "Optical coherence tomography in the gastrointestinal tract," *Endoscopy* **32**(10), 796–803 (2000).

122. S. Jäckle, N. Gladkova, F. Feldchtein, A. Terentieva, B. Brand, G. Gelikonov, V. Gelikonov, A. Sergeev, A. Fritscher-Ravens, J. Freund, U. Seitz, S. Schröder, and N. Soehendra, "In vivo endoscopic optical coherence tomography of the human gastrointestinal tract–toward optical biopsy," *Endoscopy* **32**(10), 743–749 (2000).

123. C. Pitris, C. Jesser, S. A. Boppart, D. Stamper, M. E. Brezinski, and J. G. Fujimoto, "Feasibility of optical coherence tomography for high-resolution imaging of human gastrointestinal tract malignancies," *J. Gastroenterol.* **35**(2), 87–92 (2000).

124. G. J. Tearney, M. E. Brezinski, J. F. Southern, B. E. Bouma, S. A. Boppart, and J. G. Fujimoto, "Optical biopsy in human gastrointestinal tissue using optical coherence tomography," *Am. J. Gastroenterol.* **92**(10), 1800–1804 (1997).

125. A. Chak, M. B. Wallace, and J. M. Poneros, "Optical coherence tomography of Barrett's esophagus," *Endoscopy* **37**(6), 587–590 (2005).

126. S. A. Faruqi, V. Arantes, and M. S. Bhutani, "Barrett's esophagus: current and future role of endosonography and optical coherence tomography," *Dis. Esophagus* **17**(2), 118–123 (2004).

127. G. Isenberg, M. V. Sivak, A. Chak, R. C. K. Wong, J. E. Willis, B. Wolf, D. Y. Rowland, A. Das, and A. Rollins, "Accuracy of endoscopic optical coherence tomography in the detection of dysplasia in Barrett's esophagus: a prospective, double-blinded study," *Gastrointest. Endosc.* **62**(6), 825–831 (2005).

128. S. Jäckle, N. Gladkova, F. Feldchtein, A. Terentieva, B. Brand, G. Gelikonov, V. Gelikonov, A. Sergeev, A. Fritscher-Ravens, J. Freund, U. Seitz, S. Schröder, and N. Soehendra, "In vivo endoscopic optical coherence tomography of esophagitis, Barrett's esophagus, and adenocarcinoma of the esophagus," *Endoscopy* **32**(10), 750–755 (2000).

129. X. D. Li, S. A. Boppart, J. Van Dam, H. Mashimo, M. Mutinga, W. Drexler, M. Klein, C. Pitris, M. L. Krinsky, M. E. Brezinski, and J. G. Fujimoto, "Optical coherence tomography: advanced technology for the endoscopic imaging of Barrett's esophagus," *Endoscopy* **32**(12), 921–930 (2000).

130. J. M. Poneros and N. S. Nishioka, "Diagnosis of Barrett's esophagus using optical coherence tomography," *Gastrointest Endosc Clin. N. Am.* **13**(2), 309–323 (2003).

131. J. Poneros, "Optical coherence tomography and the detection of dysplasia in Barrett's esophagus," *Gastrointest. Endosc.* **62**(6), 832–833 (2005).

132. X. Qi, M. V. Sivak, G. Isenberg, J. E. Willis, and A. M. Rollins, "Computer-aided diagnosis of dysplasia in Barrett's esophagus using endoscopic optical coherence tomography," *J. Biomed. Opt.* **11**(4), 044010 (2006).

133. A. Wax, J. W. Pyhtila, R. N. Graf, R. Nines, C. W. Boone, R. R. Dasari, M. S. Feld, V. E. Steele, and G. D. Stoner, "Prospective grading of neoplastic change in rat esophagus epithelium using angle-resolved low-coherence interferometry," *J. Biomed. Opt.* **10**(5), 051604 (2005).

134. P. F. Escobar, J. L. Belinson, A. White, N. M. Shakhova, F. I. Feldchtein, M. V. Kareta, and N. D. Gladkova, "Diagnostic efficacy of optical coherence tomography in the management of preinvasive and invasive cancer of uterine cervix and vulva," *Intl. J. Gynecolog. Cancer* **14**(3), 470–474 (2004).

135. R. Drezek, M. Guillaud, T. Collier, I. Boiko, A. Malpica, C. Macaulay, M. Follen, and R. Richards-Kortum, "Light scattering from cervical cells throughout neoplastic progression: influence of nuclear morphology, DNA content, and chromatin texture," *J. Biomed. Opt.* **8**(1), 7–16 (2003).

136. I. V. Turchin, E. A. Sergeeva, L. S. Dolin, V. A. Kamensky, N. M. Shakhova, and R. Richards-Kortum, "Novel algorithm of processing optical coherence tomography images for differentiation of biological tissue pathologies," *J. Biomed. Opt.* **10**(6), 064024 (2005).

137. N. D. Gladkova, G. A. Petrova, N. K. Nikulin, S. G. Radenska-Lopovok, L. B. Snopova, Y. P. Chumakov, V. A. Nasonova, V. M. Gelikonov, G. V. Gelikonov, R. V. Kuranov, A. M. Sergeev, and F. I. Feldchtein, "In vivo optical coherence tomography imaging of human skin: norm and pathology," *Skin Res. Technol.* **6**(1), 6–16 (2000).

138. C. A. Jesser, S. A. Boppart, C. Pitris, D. L. Stamper, G. P. Nielsen, M. E. Brezinski, and J. G. Fujimoto, "High resolution imaging of transitional cell carcinoma with optical coherence tomography: feasibility for the evaluation of bladder pathology," *Br. J. Radiol.* **72**(864), 1170–1176 (1999).

139. M. J. Manyak, N. D. Gladkova, J. H. Makari, A. M. Schwartz, E. V. Zagaynova, L. Zolfaghari, J. M. Zara, R. Iksanov, and F. I. Feldchtein, "Evaluation of superficial bladder transitional-cell carcinoma by optical coherence tomography," *J. Endourol* **19**(5), 570–574 (2005).

140. A. Pagnoni, A. Knuettel, P. Welker, M. Rist, T. Stoudemayer, L. Kolbe, I. Sadiq, and A. M. Kligman, "Optical coherence tomography in dermatology," *Skin Res. Technol.* **5**(2), 83–87 (1999).

141. Y. T. Pan, T. Q. Xie, C. W. Du, S. Bastacky, S. Meyers, and M. L. Zeidel, "Enhancing early bladder cancer detection with fluorescence-guided endoscopic optical coherence tomography," *Opt. Lett.* **28**(24), 2485–2487 (2003).

142. M. C. Pierce, J. Strasswimmer, B. H. Park, B. Cense, and J. F. de Boer, "Advances in optical coherence tomography imaging for dermatology," *J. Invest. Dermatol.* **123**(3), 458–463 (2004).

143. J. M. Schmitt, M. J. Yadlowsky, and R. F. Bonner, "Subsurface imaging of living skin with optical coherence microscopy," *Dermatology (Basel, Switz.)* **191**(2), 93–98 (1995).

144. Z. G. Wang, D. B. Durand, M. Schoenberg, and Y. T. Pan, "Fluorescence guided optical coherence tomography for the diagnosis of early bladder cancer in a rat model," *J. Urol. (Baltimore)* **174**(6), 2376–2381 (2005).

145. E. V. Zagaynova, O. S. Streltsova, N. D. Gladkova, L. B. Snopova, G. V. Gelikonov, F. I. Feldchtein, and A. N. Morozov, "In vivo optical coherence tomography feasibility for bladder disease," *J.*

Urol. (Baltimore) **167**(3), 1492–1496 (2002).

146. J. Welzel, E. Lankenau, R. Birngruber, and R. Engelhardt, "Optical coherence tomography of the human skin," *J. Am. Acad. Dermatol.* **37**(6), 958–963 (1997).

147. J. Welzel, "Optical coherence tomography in dermatology: a review," *Skin Res. Technol.* **7**(1), 1–9 (2001).

148. J. Welzel, C. Reinhardt, E. Lankenau, C. Winter, and H. H. Wolff, "Changes in function and morphology of normal human skin: evaluation using optical coherence tomography," *Br. J. Dermatol.* **150**(2), 220–225 (2004).

149. W. Drexler, D. Stamper, C. Jesser, X. Li, C. Pitris, K. Saunders, S. Martin, M. B. Lodge, J. G. Fujimoto, and M. E. Brezinski, "Correlation of collagen organization with polarization sensitive imaging of *in vitro* cartilage: implications for osteoarthritis," *J. Rheumatol.* **28**(6), 1311–1318 (2001).

150. X. Li, S. Martin, C. Pitris, R. Ghanta, D. L. Stamper, M. Harman, J. G. Fujimoto, and M. E. Brezinski, "High-resolution optical coherence tomographic imaging of osteoarthritic cartilage during open knee surgery," *Arthritis Res. Ther.* **7**(2), R318–R323 (2005).

151. T. Xie, S. Guo, J. Zhang, Z. Chen, and G. M. Peavy, "Determination of characteristics of degenerative joint disease using optical coherence tomography and polarization sensitive optical coherence tomography," *Lasers Surg. Med.* **38**(9), 852–865 (2006).

152. J. J. Armstrong, M. S. Leigh, I. D. Walton, A. V. Zvyagin, S. A. Alexandrov, S. Schwer, D. D. Sampson, D. R. Hillman, and P. R. Eastwood, "*In vivo* size and shape measurement of the human upper airway using endoscopic long-range optical coherence tomography," *Opt. Express* **11**(15), 1817–1826 (2003).

153. J. J. Armstrong, M. S. Leigh, D. D. Sampson, J. H. Walsh, D. R. Hillman, and P. R. Eastwood, "Quantitative upper airway imaging with anatomic optical coherence tomography," *Am. J. Respir. Crit. Care Med.* **173**(2), 226–233 (2006).

154. A. Z. Freitas, D. M. Zezell, N. D. Vieira, A. C. Ribeiro, and A. S. L. Gomes, "Imaging carious human dental tissue with optical coherence tomography," *J. Appl. Phys.* **99**(2), 024906 (2006).

155. L. L. Otis, M. J. Everett, U. S. Sathyam, and B. W. Colston, "Optical coherence tomography: A new imaging technology for dentistry," *J. Am. Dent. Assoc.* **131**(4), 511–514 (2000).

156. B. J. Tromberg, "Overcoming barriers to clinical translation," in *Optical Imaging 2006: Fifth Inter-Institute Workshop on Optical Diagnostic Imaging from Bench to Bedside at the National Institutes of Health*, Bethesda, MD (2006).

157. Cureline, Inc., see http://www.cureline.com (2007).

158. National Disease Research Exchange, see http://www.ndriresource.org (2007).

159. J. M. Crawford, "Optics and the pathology gold standard," in *Optical Imaging 2006: Fifth Inter-Institute Workshop on Optical Diagnostic Imaging from Bench to Bedside at the National Institutes of Health*, Bethesda, MD (2006).

160. D. M. Eddy, "Practice policies: where do they come from?" *JAMA, J. Am. Med. Assoc.* **263**(9), 1265 (1990).

161. M. J. McQueen, "Overview of evidence-based medicine: Challenges for evidence-based laboratory medicine," *Clin. Chem.* **47**(8), 1536–1546 (2001).

162. C. P. Price, "Evidence-based laboratory medicine: supporting decision-making," *Clin. Chem.* **46**(8), 1041–1050 (2000).

163. D. L. Sackett and R. B. Haynes, "The architecture of diagnostic research. (Evidence base of clinical diagnosis)," *Br. Med. J.* **324**(7336), 539–541 (2002).

164. "Animal welfare act of 1966 as amended 1970, 1976, 1984, 1985, 1990, 1991 and 1995" (1966).

165. "Health research extension act of 1985" (1985).

166. "Health insurance portability and accountability act of 1996" (1996).

167. J. C. Pearson, "Informatics platforms to support collaboration and drive standardization," in *Optical Imaging 2006: Fifth Inter-Institute Workshop on Optical Diagnostic Imaging from Bench to Bedside at the National Institutes of Health*, Bethesda, MD (2006).

168. "ANSI Z136.3 Safe use of lasers in health care facilities," Laser Institute of America, Orlando, FL (2005).

169. B. J. Tromberg, J. C. Pearson, J. M. Crawford, D. A. Benaron, A. Hayward, R. Waynant, and P. Barker, "Panel discussion: Translating optical technologies from benchtop to clinical standard," in *Optical Imaging 2006: Fifth Inter-Institute Workshop on Optical Diagnostic Imaging from Bench to Bedside at the National Institutes of Health*,

Bethesda, MD (2006).

170. R. Weissleder and U. Mahmood, "Molecular imaging," *Radiology* **219**(2), 316–333 (2001).

171. S. A. Boppart, A. L. Oldenburg, C. Xu, and D. L. Marks, "Optical probes and techniques for molecular contrast enhancement in coherence imaging," *J. Biomed. Opt.* **10**(4), 041208 (2005).

172. P. A. Dayton and K. W. Ferrara, "Targeted imaging using ultrasound," *J. Magn. Reson Imaging* **16**(4), 362–377 (2002).

173. P. M. Winter, A. M. Morawski, S. D. Caruthers, R. W. Fuhrhop, H. Zhang, T. A. Williams, J. S. Allen, E. K. Lacy, J. D. Robertson, G. M. Lanza, and S. A. Wickline, "Molecular imaging of angiogenesis in early-stage atherosclerosis with $\alpha v \beta 3$-integrin-targeted nanoparticles," *Circulation* **108**(18), 2270–2274 (2003).

174. F. J. J. Toublan, S. Boppart, and K. S. Suslick, "Tumor targeting by surface-modified protein microspheres," *J. Am. Chem. Soc.* **128**(11), 3472–3473 (2006).

175. S. J. Oldenburg, R. D. Averitt, S. L. Westcott, and N. J. Halas, "Nanoengineering of optical resonances," *Chem. Phys. Lett.* **288**(2), 243–247 (1998).

176. A. Agrawal, S. Huang, A. W. H. Lin, M. H. Lee, J. K. Barton, R. A. Drezek, and T. J. Pfefer, "Quantitative evaluation of optical coherence tomography signal enhancement with gold nanoshells," *J. Biomed. Opt.* **11**(4), 041121 (2006).

177. G. Kong, R. D. Braun, and M. W. Dewhirst, "Hyperthermia enables tumor-specific nanoparticle delivery: Effect of particle size," *Cancer Res.* **60**(16), 4440–4445 (2000).

178. L. R. Hirsch, R. J. Stafford, J. A. Bankson, S. R. Sershen, B. Rivera, R. E. Price, J. D. Hazle, N. J. Halas, and J. L. West, "Nanoshell-mediated near-infrared thermal therapy of tumors under magnetic resonance guidance," *Proc. Natl. Acad. Sci. U.S.A.* **100**(23), 13549–13554 (2003).

179. J. Chen, F. Saeki, B. J. Wiley, H. Cang, M. J. Cobb, Z. Y. Li, L. Au, H. Zhang, M. B. Kimmey, X. Li, and Y. Xia, "Gold nanocages: Bioconjugation and their potential use as optical imaging contrast agents," *Nano Lett.* **5**(3), 473–477 (2005).

180. A. L. Oldenburg, M. N. Hansen, D. A. Zweifel, A. Wei, and S. A. Boppart, "Plasmon-resonant gold nanorods as low backscattering albedo contrast agents for optical coherence tomography," *Opt. Express* **14**(15), 6724–6738 (2006).

181. X. Huang, I. H. El-Sayed, W. Qian, and M. A. El-Sayed, "Cancer cell imaging and photothermal therapy in the near-infrared region by using gold nanorods," *J. Am. Chem. Soc.* **128**(6), 2115–2120 (2006).

182. U. Morgner, W. Drexler, F. X. Kärtner, X. D. Li, C. Pitris, E. P. Ippen, and J. G. Fujimoto, "Spectroscopic optical coherence tomography," *Opt. Lett.* **25**(2), 111–113 (2000).

183. D. J. Faber, E. G. Mik, M. C. G. Aalders, and T. G. van Leeuwen, "Toward assessment of blood oxygen saturation by spectroscopic optical coherence tomography," *Opt. Lett.* **30**(9), 1015–1017 (2005).

184. D. C. Adler, T. H. Ko, P. R. Herz, and J. G. Fujimoto, "Optical coherence tomography contrast enhancement using spectroscopic analysis with spectral autocorrelation," *Opt. Express* **12**(22), 5487–5501 (2004).

185. C. Xu, P. S. Carney, and S. A. Boppart, "Wavelength-dependent scattering in spectroscopic optical coherence tomography," *Opt. Express* **13**(14), 5450–5462 (2005).

186. C. Xu, D. L. Marks, M. N. Do, and S. A. Boppart, "Separation of absorption and scattering profiles in spectroscopic optical coherence tomography using a least-squares algorithm," *Opt. Express* **12**(20), 4790–4803 (2004).

187. H. Cang, T. Sun, Z. Y. Li, J. Chen, B. J. Wiley, Y. Xia, and X. Li, "Gold nanocages as contrast agents for spectroscopic optical coherence tomography," *Opt. Lett.* **30**(22), 3048–3050 (2005).

188. T. Støren, A. Røyset, L. O. Svaasand, and T. Lindmo, "Functional imaging of dye concentration in tissue phantoms by spectroscopic optical coherence tomography," *J. Biomed. Opt.* **10**(2), 024037 (2005).

189. M. G. Harisinghani, J. Barentsz, P. F. Hahn, W. M. Deserno, S. Tabatabaei, C. H. van de Kaa, J. de la Rosette, and R. Weissleder, "Noninvasive detection of clinically occult lymph-node metastases in prostate cancer," *N. Engl. J. Med.* **348**(25), 2491–2499 (2003).

190. A. L. Oldenburg, F. J. J. Toublan, K. S. Suslick, A. Wei, and S. A. Boppart, "Magnetomotive contrast for *in vivo* optical coherence tomography," *Opt. Express* **13**(17), 6597–6614 (2005).

191. J. Kim, J. Oh, T. E. Milner, and J. S. Nelson, "Hemoglobin contrast in magnetomotive optical Doppler tomography," *Opt. Lett.* **31**(6),

778–780 (2006).

192. D. Artemov, N. Mori, B. Okollie, and Z. M. Bhujwalla, "MR molecular imaging of the Her-2/neu receptor in breast cancer cells using targeted iron oxide nanoparticles," *Magn. Reson. Med.* **49**(3), 403–408 (2003).

193. W. J. Rogers and P. Basu, "Factors regulating macrophage endocytosis of nanoparticles: implications for targeted magnetic resonance plaque imaging," *Atherosclerosis* **178**(1), 67–73 (2005).

194. J. Oh, M. D. Feldman, J. Kim, C. Condit, S. Emalianov, and T. E. Milner, "Detection of magnetic nanoparticles in tissue using magneto-motive ultrasound," *Nanotechnology* **17**(16), 4183–4190 (2006).

195. S. Hamaguchi, I. Tohnai, A. Ito, K. Mitsudo, T. Shigetomi, M. Ito, H. Honda, T. Kobayashi, and M. Ueda, "Selective hyperthermia using magnetoliposomes to target cervical lymph node metastasis in a rabbit tongue tumor model," *Cancer Sci.* **94**(9), 834–839 (2003).

196. B. E. Applegate, C. Yang, and J. A. Izatt, "Theoretical comparison of the sensitivity of molecular contrast optical coherence tomography techniques," *Opt. Express* **13**(20), 8146–8163 (2005).

197. B. E. Applegate and J. A. Izatt, "Molecular imaging of endogenous and exogenous chromophores using ground state recovery pump-probe optical coherence tomography," *Opt. Express* **14**(20), 9142–9155 (2006).

198. A. Zumbusch, G. R. Holtom, and X. S. Xie, "Three-dimensional vibrational imaging by coherent anti-Stokes Raman scattering," *Phys. Rev. Lett.* **82**(20), 4142–4145 (1999).

199. D. L. Marks, C. Vinegoni, J. S. Bredfeldt, and S. A. Boppart, "Interferometric differentiation between resonant coherent anti-Stokes Raman scattering and nonresonant four-wave-mixing processes," *Appl. Phys. Lett.* **85**(23), 5787–5789 (2004).

200. C. L. Evans, E. O. Potma, and X. S. Xie, "Coherent anti-Stokes Raman scattering spectral interferometry: determination of the real and imaginary components of nonlinear susceptibility chi(3) for vibrational microscopy," *Opt. Lett.* **29**(24), 2923–2925 (2004).

201. E. O. Potma, C. L. Evans, and X. S. Xie, "Heterodyne coherent anti-Stokes Raman scattering (CARS) imaging," *Opt. Lett.* **31**(2), 241–243 (2006).

202. P. R. Herz, Y. Chen, A. D. Aguirre, J. G. Fujimoto, H. Mashimo, J. Schmitt, A. Koski, J. Goodnow, and C. Petersen, "Ultrahigh resolution optical biopsy with endoscopic optical coherence tomography," *Opt. Express* **12**(15), 3532–3542 (2004).

203. M. Laubscher, M. Ducros, B. Karamata, T. Lasser, and R. Salathé, "Video-rate three-dimensional optical coherence tomography," *Opt. Express* **10**(9), 429–435 (2002).

204. N. A. Nassif, B. Cense, B. H. Park, M. C. Pierce, S. H. Yun, B. E. Bouma, G. J. Tearney, T. C. Chen, and J. F. de Boer, "*In vivo* high-resolution video-rate spectral-domain optical coherence tomography of the human retina and optic nerve," *Opt. Express* **12**(3), 367–376 (2004).

205. N. Nassif, B. Cense, B. H. Park, S. H. Yun, T. C. Chen, B. E. Bouma, G. J. Tearney, and J. F. de Boer, "*In vivo* human retinal imaging by ultrahigh-speed spectral domain optical coherence tomography," *Opt. Lett.* **29**(5), 480–482 (2004).

206. N. Nishizawa, Y. Chen, P. Hsiung, E. P. Ippen, and J. G. Fujimoto, "Real-time, ultrahigh-resolution, optical coherence tomography with an all-fiber, femtosecond fiber laser continuum at 1.5 μm," *Opt. Lett.* **29**(24), 2846–2848 (2004).

207. B. H. Park, M. C. Pierce, B. Cense, and J. F. de Boer, "Real-time multi-functional optical coherence tomography," *Opt. Express* **11**(7), 782–793 (2003).

208. A. M. Rollins, R. Ung-arunyawee, A. Chak, R. C. K. Wong, K. Kobayashi, M. V. Sivak, and J. A. Izatt, "Real-time *in vivo* imaging of human gastrointestinal ultrastructure by use of endoscopic optical coherence tomography with a novel efficient interferometer design," *Opt. Lett.* **24**(19), 1358–1360 (1999).

209. A. M. Rollins, M. D. Kulkarni, S. Yazdanfar, R. Ung-arunyawee, and J. A. Izatt, "*In vivo* video rate optical coherence tomography," *Opt. Express* **3**(6), 219–229 (1998).

210. M. V. Sarunic, B. E. Applegate, and J. A. Izatt, "Real-time quadrature projection complex conjugate resolved Fourier domain optical coherence tomography," *Opt. Lett.* **31**(16), 2426–2428 (2006).

211. M. Wojtkowski, T. Bajraszewski, P. Targowski, and A. Kowalczyk, "Real-time *in vivo* imaging by high-speed spectral optical coherence tomography," *Opt. Lett.* **28**(19), 1745–1747 (2003).

212. V. X. D. Yang, M. L. Gordon, B. Qi, J. Pekar, S. Lo, E. Seng-Yue, A. Mok, B. C. Wilson, and I. A. Vitkin, "High speed, wide velocity dynamic range Doppler optical coherence tomography (Part I): system design, signal processing, and performance," *Opt. Express* **11**(7), 794–809 (2003).

213. A. V. Zvyagin, J. B. FitzGerald, K. K. M. B. D. Silva, and D. D. Sampson, "Real-time detection technique for Doppler optical coherence tomography," *Opt. Lett.* **25**(22), 1645–1647 (2000).

214. A. F. Fercher, C. K. Hitzenberger, G. Kamp, and S. Y. El-Zaiat, "Measurement of intraocular distances by backscattering spectral interferometry," *Opt. Commun.* **117**(1–2), 43–48 (1995).

215. G. Häusler and M. W. Lindner, "'Coherence' radar and 'spectral radar'—New tools for dermatological diagnosis," *J. Biomed. Opt.* **3**(1), 21–31 (1998).

216. R. A. Leitgeb, W. Drexler, A. Unterhuber, B. Hermann, T. Bajraszewski, T. Le, A. Stingl, and A. F. Fercher, "Ultrahigh-resolution Fourier domain optical coherence tomography," *Opt. Express* **12**(10), 2156–2165 (2004).

217. M. Wojtkowski, V. J. Srinivasan, T. H. Ko, J. G. Fujimoto, A. Kowalczyk, and J. S. Duker, "Ultrahigh-resolution, high-speed, Fourier domain optical coherence tomography and methods for dispersion compensation," *Opt. Express* **12**(11), 2404–2422 (2004).

218. C. Xu, C. Vinegoni, T. S. Ralston, W. Luo, W. Tan, and S. A. Boppart, "Spectroscopic spectral-domain optical coherence microscopy," *Opt. Lett.* **31**(8), 1079–1081 (2006).

219. S. H. Yun, G. J. Tearney, B. E. Bouma, B. H. Park, and J. F. de Boer, "High-speed spectral-domain optical coherence tomography at 1.3 μm wavelength," *Opt. Express* **11**(30), 3598–3604 (2003).

220. P. Blazkiewicz, M. Gourlay, J. R. Tucker, A. D. Rakic, and A. V. Zvyagin, "Signal-to-noise ratio study of full-field Fourier-domain optical coherence tomography," *Appl. Opt.* **44**(36), 7722–7729 (2005).

221. J. F. de Boer, B. Cense, B. H. Park, M. C. Pierce, G. J. Tearney, and B. E. Bouma, "Improved signal-to-noise ratio in spectral-domain compared with time-domain optical coherence tomography," *Opt. Lett.* **28**(21), 2067–2069 (2003).

222. R. Leitgeb, C. K. Hitzenberger, and A. F. Fercher, "Performance of fourier domain vs. time domain optical coherence tomography," *Opt. Express* **11**(8), 889–894 (2003).

223. S. R. Chinn, E. A. Swanson, and J. G. Fujimoto, "Optical coherence tomography using a frequency-tunable optical source," *Opt. Lett.* **22**(5), 340–342 (1997).

224. M. A. Choma, M. V. Sarunic, C. Yang, and J. A. Izatt, "Sensitivity advantage of swept source and Fourier domain optical coherence tomography," *Opt. Express* **11**(18), 2183–2189 (2003).

225. B. Golubovic, B. E. Bouma, G. J. Tearney, and J. G. Fujimoto, "Optical frequency-domain reflectometry using rapid wavelength tuning of a Cr4+:forsterite laser," *Opt. Lett.* **22**(22), 1704–1706 (1997).

226. U. H. P. Haberland, V. Blazek, and H. J. Schmitt, "Chirp optical coherence tomography of layered scattering media," *J. Biomed. Opt.* **3**(3), 259–266 (1998).

227. R. Huber, M. Wojtkowski, J. G. Fujimoto, J. Y. Jiang, and A. E. Cable, "Three-dimensional and C-mode OCT imaging with a compact, frequency swept laser source at 1300 nm," *Opt. Express* **13**(26), 10523–10538 (2005).

228. R. Huber, M. Wojtkowski, and J. G. Fujimoto, "Fourier Domain Mode Locking (FDML): A new laser operating regime and applications for optical coherence tomography," *Opt. Express* **14**(8), 3225–3237 (2006).

229. R. Huber, D. C. Adler, and J. G. Fujimoto, "Buffered Fourier domain mode locking: unidirectional swept laser sources for optical coherence tomography imaging at 370,000 lines/s," *Opt. Lett.* **31**(20), 2975–2977 (2006).

230. S. Moon and D. Y. Kim, "Ultra-high-speed optical coherence tomography with a stretched pulse supercontinuum source," *Opt. Express* **14**(24), 11575–11584 (2006).

231. M. D. Kulkarni and J. A. Izatt, "Digital signal processing in optical coherence tomography," *Proc. SPIE* **2981**, pp. 2–6 (1997).

232. H. E. Larsen, R. T. Nilsson, L. Thrane, D. K. Kristensen, F. Pedersen, T. M. Jorgensen, A. Gualdino, and P. E. Andersen, "Optical Doppler coherence tomography based on a field-programmable gate array," *Proc. SPIE* **5690**, pp. 263–270 (2005).

233. S. Yan, D. Piao, Y. Chen, and Q. Zhu, "DSP-based optical Doppler tomography system for real-time signal processing," *Proc. SPIE* **4956**, pp. 187–196 (2003).

234. S. Yan, D. Piao, Y. Chen, and Q. Zhu, "Digital signal processor-based real-time optical Doppler tomography system," *J. Biomed. Opt.* **9**(3), 454–463 (2004).

235. T. S. Ralston, J. A. Mayen, D. L. Marks, and S. A. Boppart, "Real-time digital design for an optical coherence tomography acquisition and processing system," *Proc. SPIE* **5324**, pp. 159–170 (2004).

236. A. W. Schaefer, J. J. Reynolds, D. L. Marks, and S. A. Boppart, "Real-time digital signal processing-based optical coherence tomography and Doppler optical coherence tomography," *IEEE Trans. Biomed. Eng.* **51**(1), 186–190 (2004).

237. V. Westphal, S. Yazdanfar, A. M. Rollins, and J. A. Izatt, "Real-time, high velocity-resolution color Doppler optical coherence tomography," *Opt. Lett.* **27**(1), 34–36 (2002).

238. M. Pircher, E. Goetzinger, R. Leitgeb, and C. K. Hitzenberger, "Three dimensional polarization sensitive OCT of human skin in vivo," *Opt. Express* **12**(14), 3236–3244 (2004).

239. B. M. Hoeling, A. D. Fernandez, R. C. Haskell, E. Huang, W. R. Myers, D. C. Petersen, S. E. Ungersma, R. Wang, M. E. Williams, and S. E. Fraser, "An optical coherence microscope for 3-dimensional imaging in developmental biology," *Opt. Express* **6**(7), 136–146 (2000).

240. P. L. Hsiung, Y. Chen, T. H. Ko, J. G. Fujimoto, C. J. S. de Matos, S. V. Popov, J. R. Taylor, and V. P. Gapontsev, "Optical coherence tomography using a continuous-wave, high-power, Raman continuum light source," *Opt. Express* **12**(22), 5287–5295 (2004).

241. C. Xi, D. L. Marks, D. S. Parikh, L. Raskin, and S. A. Boppart, "Structural and functional imaging of 3D microfluidic mixers using optical coherence tomography," *Proc. Natl. Acad. Sci. U.S.A.* **101**(20), 7516–7521 (2004).

242. C. Xi, D. Marks, S. Schlachter, W. Luo, and S. A. Boppart, "High-resolution three-dimensional imaging of biofilm development using optical coherence tomography," *J. Biomed. Opt.* **11**(3), 034001 (2006).

243. T. S. Ralston, D. L. Marks, P. S. Carney, and S. A. Boppart, "Inverse scattering for optical coherence tomography," *J. Opt. Soc. Am. A Opt. Image Sci. Vis* **32**(5), 1027–1037 (2006).

244. T. S. Ralston, D. L. Marks, P. S. Carney, and S. A. Boppart, "Interferometric synthetic aperture microscopy," *Nat. Phys.* **3**(2), 129–134 (2007).

245. T. S. Ralston, D. L. Marks, S. A. Boppart, and P. S. Carney, "Inverse scattering for high-resolution interferometric microscopy," *Opt. Lett.* **31**(24), 3585–3587 (2006).

246. D. L. Marks, T. S. Ralston, P. S. Carney, and S. A. Boppart, "Inverse scattering for rotationally scanned optical coherence tomography," *J. Opt. Soc. Am. A Opt. Image Sci. Vis.* **23**(10), 2433–2439 (2006).

247. D. L. Marks, T. S. Ralston, S. A. Boppart, and P. S. Carney, "Inverse scattering for frequency-scanned full-field optical coherence tomography," *J. Opt. Soc. Am. A Opt. Image Sci. Vis.* **24**(4), 1034–1041 (2007).

248. W. Drexler, "Ultrahigh-resolution optical coherence tomography," *J. Biomed. Opt.* **9**(1), 47–74 (2004).

249. A. F. Fercher, C. K. Hitzenberger, M. Sticker, E. Moreno-Barriuso, R. Leitgeb, W. Drexler, and H. Sattmann, "A thermal light source technique for optical coherence tomography," *Opt. Commun.* **185**(1), 57–64 (2000).

250. L. Vabre, A. Dubois, and A. C. Boccara, "Thermal-light full-field optical coherence tomography," *Opt. Lett.* **27**(7), 530–532 (2002).

251. G. Moneron, A. C. Boccara, and A. Dubois, "Stroboscopic ultrahigh-resolution full-field optical coherence tomography," *Opt. Lett.* **30**(11), 1351–1353 (2005).

252. A. Baumgartner, C. K. Hitzenberger, H. Sattmann, W. Drexler, and A. F. Fercher, "Signal and resolution enhancements in dual beam optical coherence tomography of the human eye," *J. Biomed. Opt.* **3**(1), 45–54 (1998).

253. T. H. Ko, D. C. Adler, J. G. Fujimoto, D. Mamedov, V. Prokhorov, V. Shidlovski, and S. Yakubovich, "Ultrahigh resolution optical coherence tomography imaging with a broadband superluminescent diode light source," *Opt. Express* **12**(10), 2112–2119 (2004).

254. A. Unterhuber, B. Považay, B. Hermann, H. Sattmann, A. Chavez-Pirson, and W. Drexler, "In vivo retinal optical coherence tomography at 1040 nm-enhanced penetration into the choroid," *Opt. Express* **13**(9), 3252–3258 (2005).

255. A. M. Kowalevicz, T. Ko, I. Hartl, J. G. Fujimoto, M. Pollnau, and R. P. Salathé, "Ultrahigh resolution optical coherence tomography using a superluminescent light source," *Opt. Express* **10**(7), 349–353 (2002).

256. B. Bouma, G. J. Tearney, S. A. Boppart, M. R. Hee, M. E. Brezinski, and J. G. Fujimoto, "High-resolution optical coherence tomographic imaging using a mode-locked Ti:Al2O3 laser source," *Opt. Lett.* **20**(13), 1486–1488 (1995).

257. W. Drexler, U. Morgner, F. X. Kärtner, C. Petris, S. A. Boppart, X. D. Li, E. P. Ippen, and J. G. Fujimoto, "*In vivo* ultrahigh-resolution optical coherence tomography," *Opt. Lett.* **24**(17), 1221–1223 (1999).

258. A. Unterhuber, B. Považay, B. Hermann, H. Sattmann, W. Drexler, V. Yakovlev, G. Tempea, C. Schubert, E. M. Anger, P. K. Ahnelt, M. Stur, J. E. Morgan, A. Cowey, G. Jung, T. Le, and A. Stingl, "Compact, low-cost Ti:Al2O3 laser for *in vivo* ultrahigh-resolution optical coherence tomography," *Opt. Lett.* **28**(11), 905–907 (2003).

259. A. M. Kowalevicz, T. R. Schibli, F. X. Kärtner, and J. G. Fujimoto, "Ultralow-threshold Kerr-lens mode-locked Ti:Al2O3 laser," *Opt. Lett.* **27**(22), 2037–2039 (2002).

260. S. Bourquin, A. D. Aguirre, I. Hartl, P. Hsiung, T. H. Ko, J. G. Fujimoto, T. A. Birks, W. J. Wadsworth, U. Bünting, and D. Kopf, "Ultrahigh resolution real time OCT imaging using a compact femtosecond Nd:Glass laser and nonlinear fiber," *Opt. Express* **11**(24), 3290–3297 (2003).

261. P. C. Wagenblast, T. H. Ko, J. G. Fujimoto, F. X. Kaertner, and U. Morgner, "Ultrahigh-resolution optical coherence tomography with a diode-pumped broadband Cr3+:LiCAF laser," *Opt. Express* **12**(14), 3257–3263 (2004).

262. K. Bizheva, B. Považay, B. Hermann, H. Sattmann, W. Drexler, M. Mei, R. Holzwarth, T. Hoelzenbein, V. Wacheck, and H. Pehamberger, "Compact, broad-bandwidth fiber laser for sub-2-μm axial resolution optical coherence tomography in the 1300-nm wavelength region," *Opt. Lett.* **28**(9), 707–709 (2003).

263. S. A. Boppart, B. E. Bouma, C. Pitris, J. F. Southern, M. E. Brezinski, and J. G. Fujimoto, "*In vivo* cellular optical coherence tomography imaging," *Nat. Med.* **4**(7), 861–865 (1998).

264. B. E. Bouma, G. J. Tearney, I. P. Bilinsky, B. Golubovic, and J. G. Fujimoto, "Self-phase-modulated Kerr-lens mode-locked Cr:forsterite laser source for optical coherence tomography," *Opt. Lett.* **21**(22), 1839–1841 (1996).

265. D. L. Marks, A. L. Oldenburg, J. J. Reynolds, and S. A. Boppart, "Study of an ultrahigh-numerical-aperture fiber continuum generation source for optical coherence tomography," *Opt. Lett.* **27**(22), 2010–2012 (2002).

266. Y. Wang, I. Tomov, J. S. Nelson, Z. Chen, H. Lim, and F. Wise, "Low-noise broadband light generation from optical fibers for use in high-resolution optical coherence tomography," *J. Opt. Soc. Am. A Opt. Image Sci. Vis.* **22**(8), 1492–1499 (2005).

267. J. K. Ranka, R. S. Windeler, and A. J. Stentz, "Visible continuum generation in air-silica microstructure optical fibers with anomalous dispersion at 800 nm," *Opt. Lett.* **25**(1), 25–27 (2000).

268. I. Hartl, X. D. Li, C. Chudoba, R. K. Ghanta, T. H. Ko, J. G. Fujimoto, J. K. Ranka, and R. S. Windeler, "Ultrahigh-resolution optical coherence tomography using continuum generation in an air-silica micro structure optical fiber," *Opt. Lett.* **26**(9), 608–610 (2001).

269. A. D. Aguirre, N. Nishizawa, J. G. Fujimoto, W. Seitz, M. Lederer, and D. Kopf, "Continuum generation in a novel photonic crystal fiber for ultrahigh resolution optical coherence tomography at 800 nm and 1300 nm," *Opt. Express* **14**(3), 1145–1160 (2006).

270. G. Humbert, W. J. Wadsworth, S. G. Leon-Saval, J. C. Knight, T. A. Birks, P. S. J. Russell, M. J. Lederer, D. Kopf, K. Wiesauer, E. I. Breuer, and D. Stifter, "Supercontinuum generation system for optical coherence tomography based on tapered photonic crystal fibre," *Opt. Express* **14**(4), 1596–1603 (2006).

271. H. Lim, Y. Jiang, Y. Wang, Y. C. Huang, Z. Chen, and F. W. Wise, "Ultrahigh-resolution optical coherence tomography with a fiber laser source at 1 μm," *Opt. Lett.* **30**(10), 1171–1173 (2005).

272. B. Považay, K. Bizheva, A. Unterhuber, B. Hermann, H. Sattmann, A. F. Fercher, W. Drexler, A. Apolonski, W. J. Wadsworth, J. C. Knight, P. S. J. Russell, M. Vetterlein, and E. Scherzer, "Submicrometer axial resolution optical coherence tomography," *Opt. Lett.* **27**(20), 1800–1802 (2002).

273. B. Považay, K. Bizheva, B. Hermann, A. Unterhuber, H. Sattmann, A. F. Fercher, W. Drexler, C. Schubert, P. K. Ahnelt, M. Mei, R. Holzwarth, W. J. Wadsworth, J. C. Knight, and P. S. J. Russel, "Enhanced visualization of choroidal vessels using ultrahigh resolu-

tion ophthalmic OCT at 1050 nm," *Opt. Express* **11**(17), 1980–1986 (2003).

274. Y. Wang, Y. Zhao, J. S. Nelson, Z. Chen, and R. S. Windeler, "Ultrahigh-resolution optical coherence tomography by broadband continuum generation from a photonic crystal fiber," *Opt. Lett.* **28**(3), 182–184 (2003).

275. S. H. Yun, G. J. Tearney, J. F. de Boer, N. Iftimia, and B. E. Bouma, "High-speed optical frequency-domain imaging," *Opt. Express* **11**(22), 2953–2963 (2003).

276. S. H. Yun, G. J. Tearney, J. F. de Boer, and B. E. Bouma, "Pulsed-source and swept-source spectral-domain optical coherence tomography with reduced motion artifacts," *Opt. Express* **12**(23), 5614–5624 (2004).

277. M. A. Choma, K. Hsu, and J. A. Izatt, "Swept source optical coherence tomography using an all-fiber 1300-nm ring laser source," *J. Biomed. Opt.* **10**(4), 044009 (2005).

278. R. Huber, M. Wojtkowski, K. Taira, J. G. Fujimoto, and K. Hsu, "Amplified, frequency swept lasers for frequency domain reflecto-metry and OCT imaging: design and scaling principles," *Opt. Express* **13**(9), 3513–3528 (2005).

279. Y. Yasuno, V. D. Madjarova, S. Makita, M. Akiba, A. Morosawa, C. Chong, T. Sakai, K. P. Chan, M. Itoh, and T. Yatagai, "Three-dimensional and high-speed swept-source optical coherence tomography for *in vivo* investigation of human anterior eye segments," *Opt. Express* **13**(26), 10652–10664 (2005).

280. E. C. W. Lee, J. F. de Boer, M. Mujat, H. Lim, and S. H. Yun, "*In vivo* optical frequency domain imaging of human retina and choroid," *Opt. Express* **14**(10), 4403–4411 (2006).

281. H. Lim, M. Mujat, C. Kerbage, E. C. W. Lee, Y. Chen, T. C. Chen, and J. F. de Boer, "High-speed imaging of human retina *in vivo* with swept-source optical coherence tomography," *Opt. Express* **14**(26), 12902–12908 (2006).

282. H. Lim, J. F. de Boer, B. H. Park, E. C. W. Lee, R. Yelin, and S. H. Yun, "Optical frequency domain imaging with a rapidly swept laser in the 815–870 nm range," *Opt. Express* **14**(13), 5937–5944 (2006).